

CLEAN RESOURCES FINAL REPORT PACKAGE

Project proponents are required to submit a Final Report Package, consisting of a Final Public Report and a Final Financial Report. These reports are to be provided under separate cover at the conclusion of projects for review and approval by Alberta Innovates (AI) Clean Resources Division. Proponents will use the two templates that follow to report key results and outcomes achieved during the project and financial details. The information requested in the templates should be considered the minimum necessary to meet AI reporting requirements; proponents are highly encouraged to include other information that may provide additional value, including more detailed appendices. Proponents must work with the AI Project Advisor during preparation of the Final Report Package to ensure submissions are of the highest possible quality and thus reduce the time and effort necessary to address issues that may emerge through the review and approval process.

Final Public Report

The Final Public Report shall outline what the project achieved and provide conclusions and recommendations for further research inquiry or technology development, together with an overview of the performance of the project in terms of process, output, outcomes and impact measures. The report must delineate all project knowledge and/or technology developed and must be in sufficient detail to permit readers to use or adapt the results for research and analysis purposes and to understand how conclusions were arrived at. It is incumbent upon the proponent to ensure that the Final Public Report **is free of any confidential information or intellectual property requiring protection**. The Final Public Report will be released by Alberta Innovates after the confidentiality period has expired as described in the Investment Agreement.

Final Financial Report

The Final Financial Report shall provide complete and accurate accounting of all project expenditures and contributions over the life of the project pertaining to Alberta Innovates, the proponent, and any project partners. The Final Financial Report will not be publicly released.

Alberta Innovates is governed by FOIP. This means Alberta Innovates can be compelled to disclose the information received under this Application, or other information delivered to Alberta Innovates in relation to a Project, when an access request is made by anyone in the general public.

In the event an access request is received by Alberta Innovates, exceptions to disclosure within FOIP may apply. If an exception to disclosure applies, certain information may be withheld from disclosure. Applicants are encouraged to familiarize themselves with FOIP. Information regarding FOIP can be found at <http://www.servicealberta.ca/foip/>. Should you have any questions about the collection of this information, you may contact the Manager, Grants Administration Services at 780-450-5551.

CLEAN RESOURCES FINAL PUBLIC REPORT TEMPLATE

1. PROJECT INFORMATION:

Project Title:	Low-cost Process of Converting Asphaltene into Valuable Graphene-like Materials
Alberta Innovates Project Number:	IHP-BBC-2521
Submission Date:	Nov 8, 2021
Total Project Cost:	464,786
Alberta Innovates Funding:	172,000
AI Project Advisor:	Murray Gray

2. APPLICANT INFORMATION:

Applicant (Organization):	University of Alberta
Address:	12 floor DICE, 9211-116 St. NW, Edmonton, AB T6G 1H9
Applicant Representative Name:	Zhi Li
Title:	Adjunct Professor
Phone Number:	(780)492-1248
Email:	Zhi.li@ualberta.ca

Alberta Innovates and Her Majesty the Queen in right of Alberta make no warranty, express or implied, nor assume any legal liability or responsibility for the accuracy, completeness, or usefulness of any information contained in this publication, nor for any use thereof that infringes on privately owned rights. The views and opinions of the author expressed herein do not reflect those of Alberta Innovates or Her Majesty the Queen in right of Alberta. The directors, officers, employees, agents and consultants of Alberta Innovates and The Government of Alberta are exempted, excluded and absolved from all liability for damage or injury, howsoever caused, to any person in connection with or arising out of the use by that person for any purpose of this publication or its contents.

3. PROJECT PARTNERS

Please provide an acknowledgement statement for project partners, if appropriate.

RESPOND BELOW

This project is also supported by IOSI and NSERC CRD program.

A. EXECUTIVE SUMMARY

Provide a high-level description of the project, including the objective, key results, learnings, outcomes and benefits.

RESPOND BELOW

Graphene is an allotrope of carbon consisting of a single layer of carbon atoms arranged in honeycomb lattice. Due to its excellent flexibility, conductivity and mechanical strength, graphene has found wide applications in electronics, energy storage and reinforcement in composite materials. Despite of the performance boosts achieved with graphene, its high processing cost obstructs its large-scale applications. The current price of high-quality graphene materials is ~\$50,000/kg with a market size of \$ 200M by 2020. It is highly desirable to develop a low-cost graphene-like carbon material that can be mass produced.

Asphaltenes rejected in bitumen extraction or upgrading processes in oil sands industry usually has extremely low or zero value. Asphaltenes are a class of molecules consisted of locally peri-condensed aromatic nuclei and heteroatom-rich aliphatic side chains. Considerable energy is required to break the aromatic nuclei into lighter fractions for fuel application. Instead, we developed a green, scalable and economic process of converting asphaltenes into graphene-like carbon nanomaterials with a market value up to ~\$50/g. As feedstock to make carbon materials, the aromatic nuclei in asphaltenes become an essential advantage: it minimizes the C-C bonds reconstruction requirements in the formation of the graphitic structure.

The graphene-like carbon nanosheets developed in this project exhibits excellent electrochemical performance as anode for batteries and also electrocatalytic activities in oxygen reduction and Li-S batteries due to the sulfur and natural metal single atoms inherited from asphaltene. The asphaltene “upgrading” technology developed in this project could provide Canada’s oil sands industry with a high value-added solution of asphaltene. The successful development of this disruptive technology would enable the mass production of graphene-like carbons at significantly lower cost compared to the widely used chemical vapor deposition (CVD) method and graphite-exfoliation method.

B. INTRODUCTION

Please provide a narrative introducing the project using the following sub-headings.

- **Sector introduction:** Include a high-level discussion of the sector or area that the project contributes to and provide any relevant background information or context for the project.
- **Knowledge or Technology Gaps:** Explain the knowledge or technology gap that is being addressed along with the context and scope of the technical problem.

RESPOND BELOW

- **Sector introduction**

Graphene is a 2D allotrope of carbon consisting of a single layer of carbon atoms arranged in honeycomb lattice. This unique 2D structure provides graphene with exceptional tensile strength of 130 GPa that is hundreds of times stronger than structural steels. Being a zero-overlap semimetal (with both holes and electrons as charge carriers), graphene possesses the highest known thermal and electrical conductivity. Two routes have been developed to fabricate graphene in the past decade. The first route is chemical vapor deposition (CVD) on copper or nickel foils (catalysts) using methane as carbon source. The operation needs to be carried out in high-vacuum and at over 1000°C. Only one piece of graphene can be obtained from each foil after etching away the metal foil. Although the CVD graphene is often with good quality and large size, its cost is also extremely high. The second route is based on the exfoliation of graphite, also known as Hummers' method. The graphite is firstly oxidized into graphene oxide with different thickness under an extremely oxidative environment involving KMnO_4 and concentrated HNO_3 . The thin graphene oxide layers are separated from the thick ones through multi-step centrifugation and then reduced to graphene. This type of graphene costs significant less than CVD graphene and has found wide potential applications in various batteries and supercapacitors.⁴ However, its price tag is still very steep (over \$50/g or \$50,000,000/ton) compared to traditional carbon materials, such as graphite (~\$1,000/ton) and activated carbons (~\$20,000/ton). The high price of graphene hinders its large-scale applications, but also provides researchers with a tremendous headroom to develop some graphene alternatives from agricultural or petroleum by-products.

We are one of the pioneer research groups who realized the opportunities in agricultural by-products as feedstock for graphene-like carbon materials. Inspired by the layered structures of hemp fibre (inset of Figure 1B) which is similar to graphite, we have exfoliated and carbonized the hemp fibre, resulting in thin carbon nanosheets (**Figure 1B**) with similar morphology to graphene (**Figure 1A**). With excellent electrochemical performance and a fraction of the cost of graphene, the carbon nanosheets have received great attention from both academia and industry. It has been cited more than 380 times and featured by *BBC news* and *Chemical & Engineering News*. The related patent won 2017 TEC Edmonton Innovation Awards and is currently under commercialization. We learned in another previous work that the aromatic macrocyclic structures in organic compound (the inset of **Figure 1C**) is favorable to the formation of graphene-like carbon (**Figure 1C**).

The molecular structure of asphaltene (**Figure 1D**) is composed of several macrocyclic structures, which makes it an ideal precursor for fabricating graphene-like carbons. Firstly, the layout of carbon atoms in the polycyclic aromatic rings of asphaltene is nearly identical to that in graphene. After hydrogen atoms being cleaved off in the carbonization process, it turns into graphene small patches. The followed C-C bond reconfiguration just needs to “stitch” these patches together, which ensures the perfection and efficiency in graphitic structure formation. Secondly, the strong affinity between asphaltene and solid surfaces ensures the firm adsorption of asphaltene molecules along the solid surface, which leads to the formation of carbon in a 2D manner. Thirdly, asphaltene is rich in heteroatoms (e.g., S and N). When burned as fuel, these heteroatoms are converted into harmful SO_2 and NO_x gases which cause acid rains and damage the ozone shield in atmosphere. However, if properly preserved in carbonization process, these heteroatoms can break the electroneutralities of carbon frame and make the resulting graphene-like materials electrochemically more active for supercapacitors and electrocatalysis applications.

- Knowledge or Technology Gaps**

A few studies from other research groups have demonstrated the possibility to derive thin carbon films from coal or petroleum asphaltene feeds. However, the methods in those studies require expensive sacrificing nanoscale templates (even graphene itself) and often involve harsh chemicals (e.g., HF) to remove the templates. It is impractical in consideration of scalability and economic feasibility. Herein, we propose to develop a scalable and sustainable process to fabricate graphene using solvable salts as substrates/templates. As shown in **Figure 1E-F**, we have demonstrated the feasibility in bench-top preliminary experiments before the project.

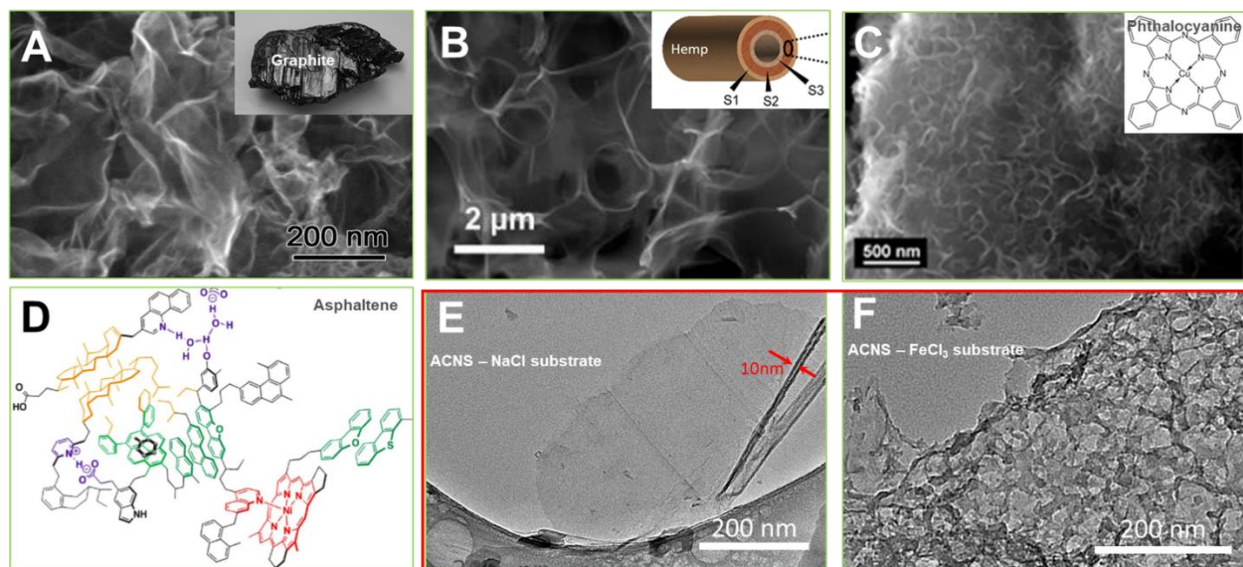


Figure 1. The graphene and graphene-like carbon nanomaterials fabricated in our previous work. A) Graphene prepared by exfoliating graphite (Nano Energy 2015, 15, 369); B) graphene-like carbon nanosheets prepared by utilizing the layered structure of hemp bast fibre (ACS Nano 2013, 7, 5131); C) graphene sponge obtained by carbonizing phthalocyanine, an aromatic macrocyclic organic compound (J. Phys. Chem. Lett. 2012, 3 2928); D) the typical molecular depiction of asphaltene (Energy & Fuels

2011, 25, 3125). The insets in A-C show the structures of precursors. E, F) The carbon nanosheets fabricated by carbonizing the asphaltene thin layer adopted on NaCl (E) and FeCl₃ (F) substrates. Due to the reactive nature of FeCl₃ (converted into FeCl₂) at high temperature, the carbon nanosheets obtained on FeCl₃ possess holey structure.

C. PROJECT DESCRIPTION

Please provide a narrative describing the project using the following sub-headings.

- **Knowledge or Technology Description:** Include a discussion of the project objectives.
- **Updates to Project Objectives:** Describe any changes that have occurred compared to the original objectives of the project.
- **Performance Metrics:** Discuss the project specific metrics that will be used to measure the success of the project.

RESPOND BELOW

The project is aimed to develop a scalable and low-cost procedure to convert asphaltenes into graphene-like carbon nanosheets, targeting at the fast-expanding energy storage market. Our scientific goal is to achieve as thin as possible carbon nanosheets for the maximal value, ideally with thickness less than 2 nm. From the view of practical applications, even the thickness of obtained nanosheets is in the range of 10-20 nm (similar to the ones derived from hemp in **Figure 1B**), they will still find wide applications in energy storage, reinforcement additives and water treatment. The objectives of the project include,

- Identify the influence of solvents, temperature, concentrations on the adsorption of asphaltenes on various substrates.
- Establish an optimized carbonization procedure to synthesize graphene-like carbon nanosheets from asphaltene in laboratory.
- Demonstrate the economic feasibility to produce different grade (thickness) carbon nanosheets.

D. METHODOLOGY

Please provide a narrative describing the methodology and facilities that were used to execute and complete the project. Use subheadings as appropriate.

RESPOND BELOW

1). Adsorption of asphaltene on substrate

The adsorption of asphaltene on the solids surface strongly depends on the property of solids surface and the aggregation of asphaltene in solvent phase and liquid/solid interface, which is driven by multiples intermolecular forces including acid-base interactions, hydrogen bonding, metal coordination, hydrophobic interactions and aromatic stacking. The locally uniform adsorption of asphaltenes on

substrate in few-layer or ideally single-layer manner directly determines the quality and thickness of ending products.

We utilized the ball milling procedure to disperse and coat asphaltene on the NaCl template. The ball-milling method is widely used in preparing active materials for energy storage with advantages including low cost in setup and precursors, efficient and scalable process and eco-friendliness.¹⁻⁴ NaCl (bulk modulus, $K_{\text{NaCl}}=24.4$ GPa, Shear modulus, $G_{\text{NaCl}}=12.61$ GPa) as the “harder” material in the system is fragmented rather than cold welded, forming fine particles. In contrast, the much “softer” asphaltene nanoaggregates in toluene, are “welded” onto the NaCl surfaces to generate stable asphaltene coated fine particles as an intermediate product before carbonized ANC is synthesized.

In a typical experiment, 200 g NaCl, 10 g of asphaltene and 20 mL toluene were placed in an agate bowl ($V_{\text{Jar}} = 500$ mL, $d_{\text{Jar}} = 100$ mm) together with 100 agate milling balls ($d_{\text{Ball}} = 20$ mm) and processed at 350 RPM for 800 minutes following a 10 minutes milling/5 minutes pausing protocol on a Fritsch Pulverisette 6 mill (Fritsch GmbH, Germany). The 20 mL toluene is the minimal amount to lubricate the milling process. No free running liquid was observed after milling. The as-prepared samples were dried in the fume hood after the ball milling finished.

2). Carbonization

As shown in **Figure 1D**, asphaltenes are primarily composed of aromatic units which are randomly oriented and joined three-dimensionally through ether and C-C bonds on side chains. In the carbonization process, the aromatic rings first lose hydrogen and peri-condensed into small carbon patches containing ~90% of carbon at 430-550 °C. However, the complex side chains and the random orientation of aromatic units prevent these patches from getting close enough to form the perfect graphitic structure. Instead, the direct carbonization of such structure often results highly distorted carbon. A significant amount of energy (i.e. high temperature) is required to smooth out the distortion and defects in the following annealing process. When asphaltenes are confined on a surface, the distortion in the carbonization process could be overcome to a large extent. Based on density-functional theory calculation, the aromatic rings are the active sites for the adsorption on various substrates. Provided with the strong affinity to substrate, the asphaltene molecular will likely adsorb on the surface with most aromatic units in semi-parallel to the substrate, which also minimizes the total surface energy of system. Compared to the randomly oriented ones, these semi-parallel aromatic units significantly diminish the possible distortion and defects in carbonization. In addition, the affinity (bonding) with substrate may even lower the activation energy required for cleaving off C-H bonds and reconfigure C-C bonds.

The ball-milled samples were carbonized using a tubular furnace (GSL-1100X, MTI) at 750 °C for 3 hours with 100 sccm argon (Ar) flow to obtain the carbonized asphaltene-derived nanostructures (ANC). The ANC material was then washed with water to remove the NaCl and then further purified with 6 M HCl, 2 M NaOH, and MilliQ water to remove any excess impurities before characterization and electrochemical tests. The NaCl can be recycled as needed. For instance, when the asphaltene/NaCl weight ratio of 1/ 20 is used, 10 g asphaltene can be processed in the 500 mL bowl, resulting in ~6 g ANC-750 after carbonization. After removing the NaCl template, the ANC was further calcined at temperatures from 900

to 1200 °C to optimize the performance as KIB anode material. The calcined ANC samples are noted as ANC-T where T is the calcination temperature.

To compare and highlight the mechanical ball milling process, we also prepared ANC in an adsorption approach with NaCl template. Asphaltene (10 wt.% toluene solution) was refluxed at 100 °C with the ball-milled NaCl in the same 1/20 ratio for 800 minutes before removing the excess toluene. The as-prepared sample was carbonized washed and characterized. Asphaltene precursor is also directly carbonized and calcined at various temperatures as reference samples (Denoted as DCA-T, T is the calcination temperature).

3). Characterization

Scanning electron microscopy (SEM) was performed using a Zeiss Sigma field-emission SEM (FESEM). Scanning helium ion microscopy (HiM) analysis was performed using a Zeiss Orion NanoFAB equipped with Ga-FIB. Transmission electron microscopy (TEM) and energy dispersive spectroscopy (EDS) analysis were performed using a JEOL ARM200 TEM, at a 200 kV accelerating voltage. Atomic force microscopy (AFM) topography and adhesion force characterization was performed using the Peak Force Quantitative Nanomechanical (PF-QNM) mode with Bruker Dimension Icon instrument equipped with an SNL-10 probe ($k=0.34 \text{ N m}^{-1}$). XPS spectra were collected with an AXIS Ultra spectrometer (Kratos Analytical Ltd, UK). The elemental content of the materials was quantified by a Flash 2000 CHNS Analyzer (Thermo Fisher Scientific).

The Raman spectra were recorded with a confocal microprobe Raman system (Renishaw inVia Qontor Confocal Raman Microscope). Typically, graphene-like materials possess two peaks as D-band and G-band at ~ 1350 and $\sim 1590 \text{ cm}^{-1}$, respectively. The D-band represents a ring breathing mode from sp^2 carbon rings which is associated with defects or graphene edges, while the G-band represents the in-plane vibrational of the sp^2 carbon in the graphene sheet. X-ray diffraction was analyzed with a Bruker Discover D8. The porosity of ANC and reference materials were characterized by N_2 adsorption at 77K (Quantachrome Autosorb iQ).

4). Electrochemical (EC) Performance Test

Coin cell type energy storage devices were fabricated and as prototype to evaluate the electrochemical performance of carbon nanosheets as anode of Li/Na/K batteries. The electrode materials were prepared by mixing the active material (ANC) with 10 wt% conductive agents (Super P) and 10 wt% binder (PVDF) in N-methylpyrrolidone (NMP) to form homogeneous slurry. The well-mixed slurry was then spread onto copper foil using a doctor blade spreader and dried at 110 °C overnight in a vacuum oven. The foil with electrode materials were then punched into circular disk electrodes about 14 mm in diameter, with $\sim 1 \text{ mg cm}^{-2}$ active materials. The active electrodes, along with a polyethylene separator, the electrolytes, and K⁺/Na⁺/Li⁺ counter electrodes were assembled in an argon-filled glovebox into CR2032-type coin cells.

For Li-S battery application, the carbon nanosheets@Cel separator was prepared by simply casting the slurry containing the asphaltene-derived carbon nanosheets and polyvinylidene fluoride (PVDF) in weight ratio of 9:1 in 1-methyl-2-pyrrolidinone (NMP) solvent onto the conventional Celgard separator

membrane, and dried at 60 °C overnight. The areal mass loading of the coating layer was controlled at 0.2 mg cm⁻². The sulfur cathode (S@SP) was prepared through the melt-diffusion method. Sulfur and Super P powder were grinded in the mass ratio of 7:3 followed by annealing at 155 °C for 6 hrs under argon atmosphere. After that, the S@SP electrodes were prepared by casting the homogeneous slurry containing S@SP composite, SP, and PVDF in the mass ratio of 8:1:1 in NMP solvent on aluminum foil and further dried at 60 °C overnight. The areal sulfur loading for regular electrodes was controlled at around 1.5 mg cm⁻². CR2032-type coin cells were assembled by using the as-prepared S@SP composite electrode as the cathode, lithium foil as the anode, and different membranes (Celgard or nanosheets@Cel) as the separator. The electrolyte contains 1M bis(trifluoromethane) sulfonimide lithium (LiTFSI) in a mixture solvent of dimethoxymethane (DME) and 1,3-dioxolane (DOL) (1/1 in v/v) with 3 wt% lithium nitrate (LiNO₃) as additive.

Cyclic voltammetry (CV) and galvanostatic charge-discharge curves were collected using a Solartron 1470E Multichannel Potentiostat /Cell Test System, to investigate the specific capacity. Galvanostatic charge-discharge cycling was performed with a multichannel-current static system (LBT20084, Arbin Instruments, College Station, TX, USA).

E. PROJECT RESULTS

Please provide a narrative describing the key results using the project's milestones as sub-headings.

- Describe the importance of the key results.
- Include a discussion of the project specific metrics and variances between expected and actual performance.

RESPOND BELOW

1. Milestone 1 (Oct 31, 2019): First-generation asphaltene-derived carbon nanosheets with a thickness less than 10-20 nm.

Millstone 1 has been successfully achieved. We fabricated asphaltene-derived carbon nanosheets by using NaCl as templates, with asphaltene: NaCl ratio of 1: 20 by weight. The carbon nanosheets by templating NaCl is named as ANC-a-b, where ANC stands for asphaltene-NaCl-carbon, a is the ratio of NaCl: asphaltene and b represents the carbonization temperature. As shown in **Figure 2 a-b**, the ANC-20-750 developed a striped texture on the surface, which is likely inherited from the NaCl templates. From the TEM image in **Figure 2c**, it can be concluded that the striped texture is uniform in width and keeps parallel to each other throughout the nanosheets. According to the nanosheets with edge bending toward the beam direction, the thickness is estimated at 16 nm.

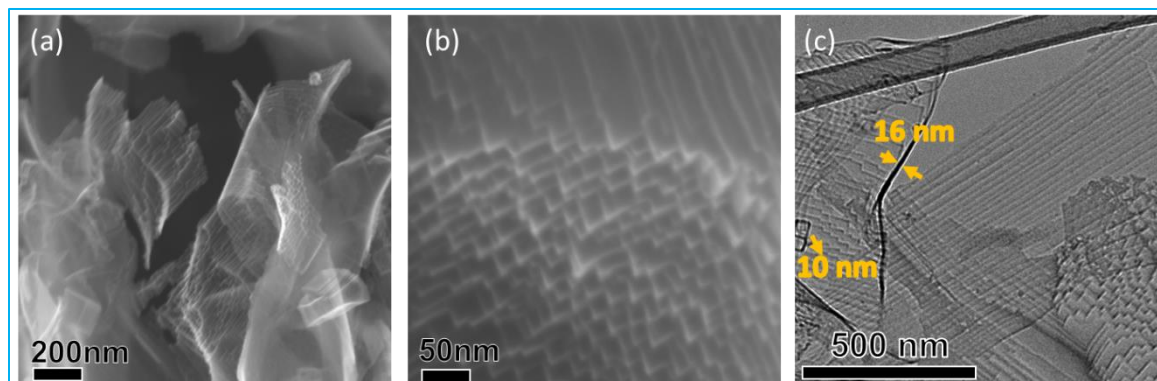


Figure 2. The morphology of ANC-20-750 by templating NaCl (asphaltene: NaCl = 1: 20 by weight). The SEM images show the thin layer structure (a) and the striped texture on the surface (b); The TEM image highlights the long-range order of the striped structure(c).

2. Milestone 2 (April 30, 2020): Second generation ACNS with a thickness less than 5 nm and electrical conductivity over 100 S m^{-1} .

By tuning the asphaltene: NaCl ratio and carbonization temperature, we have fabricated carbon nanosheets with various thickness and graphitization degree. The performance of carbon nanosheets has been evaluated as Li-ion, Na-ion, and K-ion battery electrodes. **Figure 3** shows the morphology of carbon nanosheets (ANC-200-750) carbonized at 750°C with asphaltene: NaCl ratio reduced to 1:200. The SEM image in **Figure 3a** shows the carbon layer coated NaCl crystal before washing off the template. The carbon layer is overall quite smooth on the NaCl crystal, indicating a relatively uniform coating of asphaltene before carbonization. There are some rough spots, which are likely caused by the aggregation of asphaltene. A slight edge effect can be observed, suggesting the excess buildup of asphaltene at edges and corners due to the variation in surface energy. After removing the NaCl, the thin carbon layer coated on large NaCl crystal collapsed and cracked into carbon nanosheets, which are typically a few hundred nanometers to several micrometers in size (**Figure 3b**). The striped texture can be observed. However, when the supporting NaCl crystal is small enough (less than $\sim 200 \text{ nm}$), the carbon layer can support itself after removing the NaCl template and results in a cubic carbon nanocage. As the asphaltene coating was applied at the same condition, the thickness of carbon layers on difference sized NaCl should be in the same range.

To accurately estimate the thickness of the nanosheet, at least a portion of the nanosheet needs to be in the same direction of the electron beam, otherwise, the thickness will be overestimated. However, because the nanosheets are normally lying on the TEM grid, it is difficult to find a nanosheet bends in the perfect direction. Instead, the cubic carbon cages provide a better estimation of the thickness. With one surface lying on the TEM grid, cubic cages will have four surfaces roughly in the same direction of the electron beam. According to nanocages, the thickness of carbon nanosheets is about 4 nm.

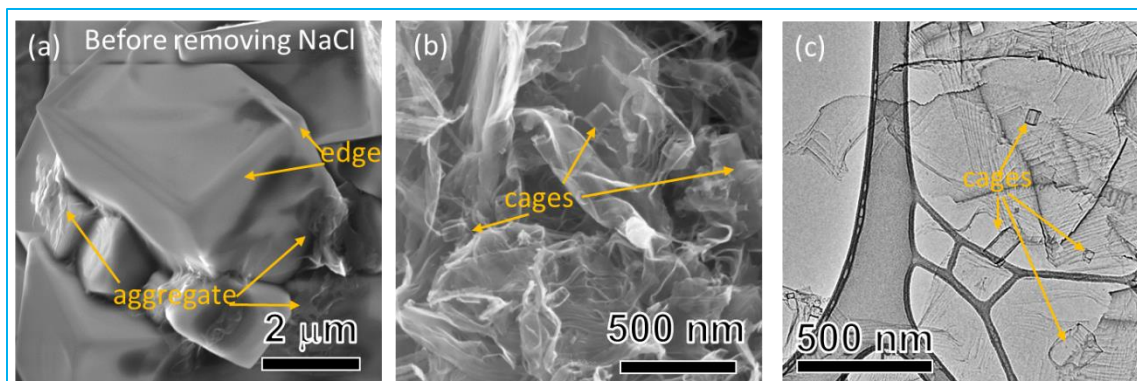


Figure 3. The morphology of ANC-200-750 by templating NaCl (asphaltene: NaCl = 1: 200 by weight). (a) The SEM image of nanosheets supported on NaCl crystal; The SEM (b) and TEM (c) image.

We found it is difficult to measure the electrical conductivity of ANC using a traditional 4-probe conductivity meter, where ANC needs to be compressed into a freestanding disc before analysis. Due to the fluffy nature of ANC, the resulting disc is highly fragile and breaks into small pieces upon contact with probes. Alternatively, we utilized a 4-probe conductivity meter specialized for powder samples. As illustrated in **Figure 4a**, continuous pressure is provided to compress the ANC powder on the 4 probes in the measurement. With the increase of the applied force, the ANC particles become better contacted, reducing overall resistance. **Figure 4b-f** shows the conductivity-pressure profiles of ANC-20 samples (NaCl: asphaltene=20:1) in comparison with lignin-derived carbon nanosheets and an electrochemical-grade activated carbon.

The conductivity of ANC exhibits a clear dependence on carbonization temperature. For example, the conductivity of ANC-20-900 (carbonized at 900°C) at 12 Mpa is ~22 S/cm (or 2,200 S/m), more than 3 time higher than electrochemical-grade activated carbon at the same condition. The conductivity can be almost doubled when the carbonization temperature increased to 1050°C (ANC-20-1050). The ANC carbonized at 750 °C possesses a conductivity of ~6.5 S/cm at 12 Mpa, only 1/3 of the ANC carbonized at 900°C, indicating the development of graphitic structure is highly dependent on the carbonization temperature. As a reference, we employed a similar procedure and made carbon nanosheets derived from lignin. Carbonized at the same temperature of 750, the conductivity of lignin-derived nanosheets is only less than 1/3 of asphaltene-derived ones, demonstrating the advantage of asphaltene over biomass precursors in forming soft and conductive carbons.

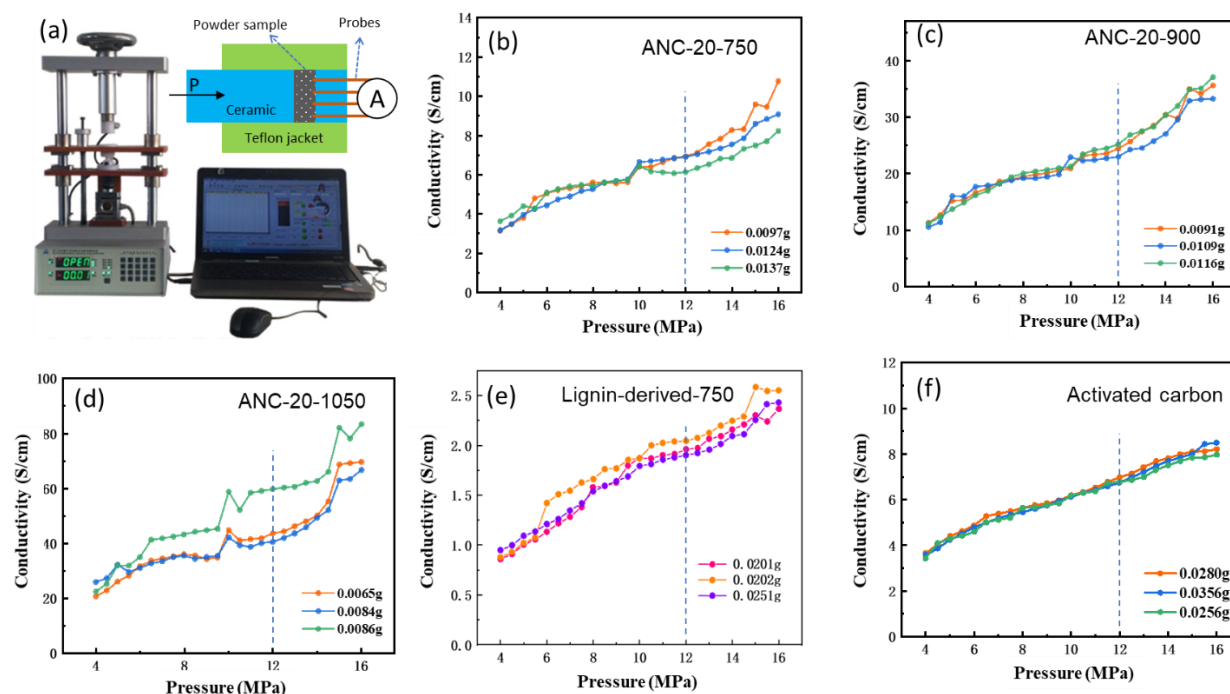


Figure 4. The conductivity of ANC in comparison with lignin-derived carbon nanosheets and activated carbon. a) The ST2722 4-probe powder sample conductivity analyzer used in this work. The conductivity-pressure profile of ANC annealed at 750 (b), 900 (c), and 1050 (d), in comparison with lignin-derived carbon nanosheets (e) and an electrochemical-grade activated carbon (f).

3. Milestone 3 (April 30, 2021): Improve the production efficiency and identify a suitable application (market sector) for ANC. ANC based coin cell batteries with 50% higher capacity than the ones using graphite as an anode at high current density or ANC based electrocatalysts with 30% higher stability than black carbon-based electrocatalysts

Milestone 3 has been successfully achieved. We have optimized the NaCl-templated carbon nanosheets for higher specific surface area and better electrochemical performance by fine-tuning the ball milling conditions and carbonization temperature. As shown in **Figure 5**, we have scaled up the procedure using a 500 ml milling bowl to process 10 g asphaltene that yielded 5.9 grams ANC-20-750 after carbonization. Due to the high specific surface area, the resulting 5.9 g ANC possesses a much higher volume than the 10 g asphaltene precursor.

The zoomed-in HiM image (**Figure 5b**) reveals the details on the wave-like surface ANC-20-900, which is consisted of a strip-like texture with a width of ~20 nm. The “strips” create a surface with multiple twists, which introduced a large amount of edge plane of the carbon nanosheets. The alternatively existing basal and edge plane on the ANC-20-900 carbon nanosheet is further characterized by atomic force microscopy (AFM) using a PeakForce QNM mode. The topographic image reveals that the strip-like structure has an average width of 20 nm (**Figure 5b**). The nanostrips aligned in an array with an 8-nm-width gap between each other to form a continuous interval sheet (red section line) and each sheet has a thickness of 5 nm

(blue section line). Considering the tip-broadening effect, the gaps contribute approximately 20% of the surface area on the carbon nanosheet. The adhesion force microscopy (**Figure 5c**) illustrates the force variation induced by the strip and the gap. The significant force changes are resultants of the orthorhombic corners of the strips. The alternatively existing stipes and gaps create densely aligned carbon edge planes.

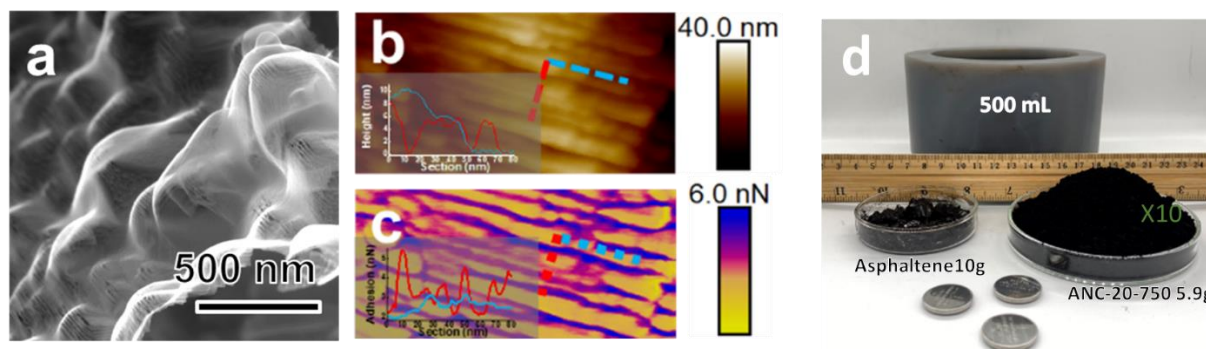


Figure 5. The morphology of ANC-20-900 by templating NaCl (asphaltene: NaCl = 1: 20 by weight). (a) The SEM (a) tomography AFM (b) and adhesion AFM (c) images of nanosheets supported on NaCl crystal; (d) the photograph of milling bowl, asphaltene and the resulting carbon nanosheets.

Table 1 listed the specific surface area of ANC-20 carbonized at a different temperature in comparison with directly carbonized asphaltene (DCA). By optimizing the ball milling conditions to achieve a uniform asphaltene coating on NaCl, the specific surface area of ANC-20-750 was improved from 95 to 268 m² g⁻¹. The increasing calcination temperature leads to the shrinking of the surface area. From ANC-20-750 to ANC-20-1200, the specific surface area characterized by Brunauer-Emmett-Teller (BET) methods decreases from 268 to 70 m² g⁻¹ with total pore volume decrease from 0.52 to 0.11 cm³ g⁻¹ (**Table 1**). Compared to that of DCA-900 (8 m² g⁻¹), the ANC-20 has the surface area increase by at least 10-fold, leading to a much-increased number of binding sites in K storage.

Table 1. The specific surface area and pore volume of ANS calculated according to BET method.

	Surface Area (m ² g ⁻¹) ^a	Pore Volume (cm ³ g ⁻¹) ^b
DCA-750	7.9	0.012
ANC-20-750	267.7	0.52
ANC-20-900	186.9	0.28
ANC-20-1050	138.2	0.19
ANC-20-1200	69.9	0.11

a. The specific surface area was calculated with Brunauer-Emmett-Teller (BET) methods; b. the total pore volume was determined at a relative pressure of 0.95.

The ANC is optimized for batteries and electrocatalysis applications. **Figure 6** shows the electrochemical performance of asphaltene-derived carbon nanosheets as anode materials for Li-ion batteries. The impact of annealing temperature was displayed in **Figure 6a** using ANC-20 as an example. The carbon nanosheets carbonized at 900°C shows the highest Li-ion storage capacity. At a low current (0.1 A g⁻¹), the capacity of ANC-20-900 is ~20% higher than that of traditional graphite. At a high current of 1 A g⁻¹, its capacity is more than 4-5 times higher than graphite.

Figure 6b shows the impact of carbon nanosheets thickness (NaCl to asphaltene ratio) on the Li-storage capacity. The thin carbon nanosheets with a NaCl to asphaltene ratio of 500 delivers the best performance. At a low current (0.1 A g⁻¹), the ANC-500-900 shows ~ 60% higher capacity than graphite. Even at an extremely high current of 20 A g⁻¹, it remains a capacity of 270 mAh g⁻¹, where the capacity of graphite becomes negligible. **Figures 6c,d** show the charge/discharge profiles of ANC at 0.1 and 1 A g⁻¹. Carbon nanosheets display typical slope discharge curves without a clear plateau, which is similar to the discharge curve of graphene but very different from the discharge curves of graphite. The results suggest that the Li ions are mainly stored on the surface or in the defects.

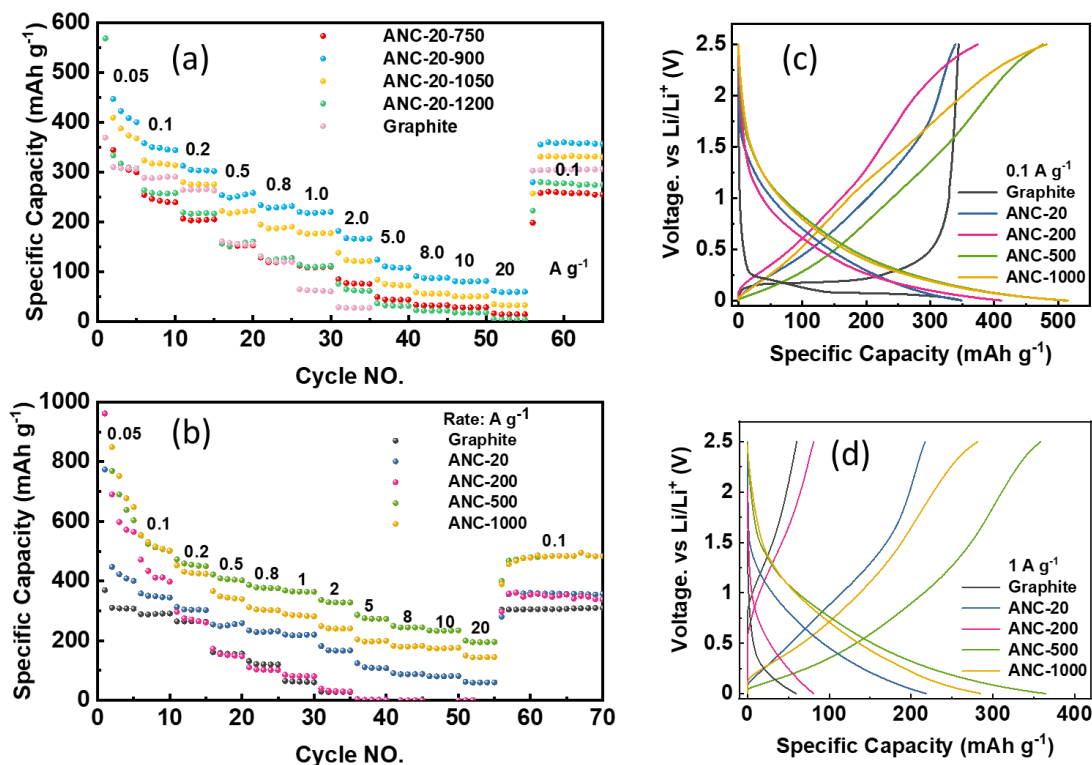


Figure 6. Li-storage performance of carbon nanosheets annealed at various temperatures (a) and with different thicknesses (b-d), in comparison with commercial graphite.

The rapidly growing energy storage demand has raised concerns about the high cost and uneven geographic distribution of lithium as an energy metal for future energy storage solutions. Sodium and potassium are sound alternatives to lithium. However, Na-ion (0.93 Å) and K-ion (1.33 Å) are significantly larger than Li-ion (0.68 Å). A K-storage capacity of $\sim 300 \text{ mAh g}^{-1}$ was achieved at 0.1 A g^{-1} with the ANC-20 sample. After optimizing the ball milling and carbonization conditions, the K-storage capacity was further improved to $\sim 400 \text{ mAh g}^{-1}$ at 0.1 A g^{-1} (**Figure 7**). At 1 A g^{-1} , the capacity was enhanced from ~ 200 to over 300 mAh g^{-1} , rendering the ANC as one of the most promising electrode materials for K-ion batteries.

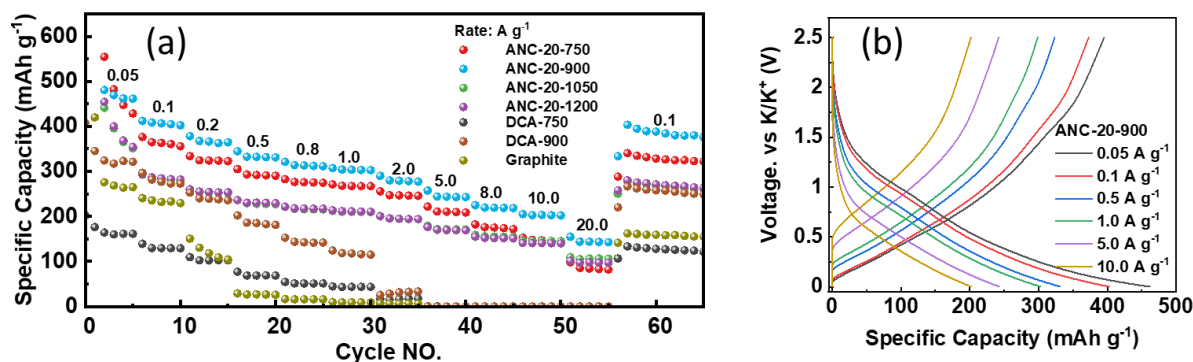


Figure 7. K-storage performance of optimized carbon nanosheets (ANC-20) annealed at various temperatures.

Besides the application in batteries, ANC can also serve as a substrate for electrocatalysts. Two Pt catalysts were prepared using ANC-200-750 as substrate. Pt NP@ANC750 stands for Pt nanoparticles (20% Pt) supported on carbon nanosheets, and Pt-SA@ANC750 represents Pt single atoms (1% Pt) dispersed on carbon nanosheets. As shown in **Figure 8a-c**, the Pt single atoms are only observable at high-resolution TEM. A high concentration of Pt atoms can be found on the edge-rich defects.

Figures 8d-f display the electrochemical oxygen reduction activity of ANC-supported Pt catalysts compared with a Pt/carbon commercial catalyst with 20% Pt (Sigma). The Pt nanoparticles supported on ANC shows similar performance to commercial Pt/carbon catalyst, promoting a 4-electron transfer reaction ($\text{O}_2 + 2\text{H}_2\text{O} + 4\text{e}^- \rightarrow 4\text{OH}^-$). In contrast, the Pt single atoms catalyst boosts the 2-electron transfer process forming hydroxide ($\text{O}_2 + \text{H}_2\text{O} + 2\text{e}^- \rightarrow \text{HO}_2^- + \text{OH}^-$). More experiments are in process to evaluate the potential of Pt-SA@ANC750 catalyst in sustainable hydrogen peroxide production, especially the role of edge-rich defects. Nevertheless, it can be concluded from the existing results that the ANC can serve as conductive substrate for electrocatalysts.

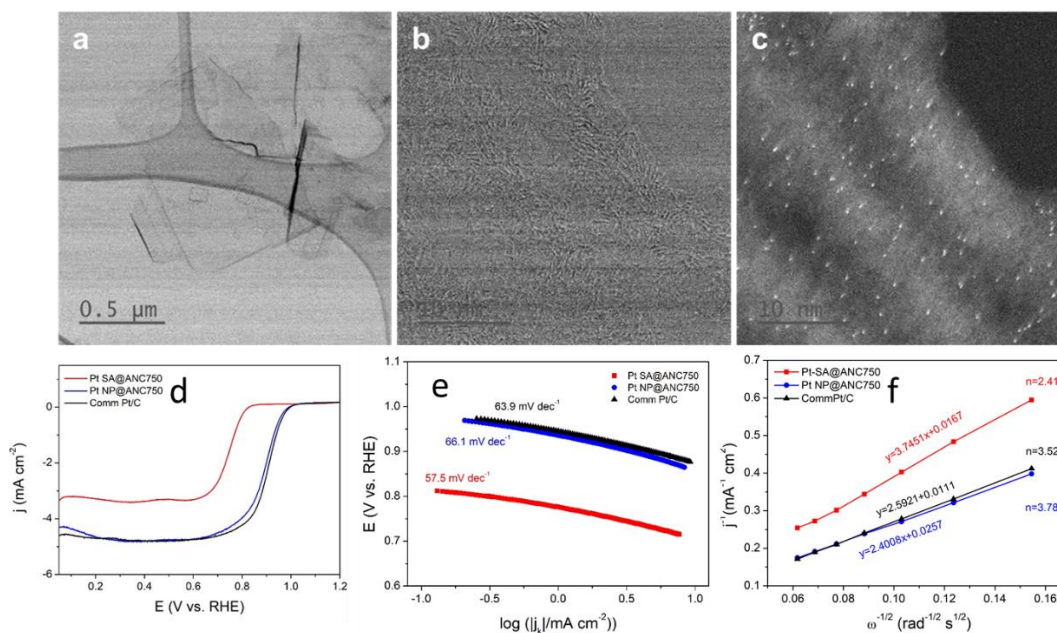


Figure 8. (a) TEM images of Pt SA@ANC750; (b,c) high-resolution BF-TEM and AC HAADF-STEM images of Pt SA@ANC750; (d) ORR polarization curves with a scanning rate of 5 mV s^{-1} for the synthesized catalysts in 0.1 M KOH solution at 1600 rpm . (e) Tafel slopes for these catalysts. (f) Koutecky-Levich plots of the synthesized catalysts at 0.6 V vs. RHE.

The advantages of ANC as anode material for Li-ion, Na-ion, and K-ion have been well demonstrated. As discussed in the previous section, ANC typically possesses 20-60% higher capacity at low current rates and 5-10 times higher capacity at high rates than graphite. That makes ANC a promising anode for high power density batteries for power tools and electrical vehicles.

4. Milestone 4 (August 31, 2021): preparation for the next phase (pilot plant) development (demonstrating the scalability, understanding the emission in production, and minimizing the energy consumption).

The regeneration of NaCl substrate and the emissions are two major sustainability concerns in the ANC production. The regeneration of NaCl substrate has been demonstrated. In our experiments, 95% of NaCl can be recycled by evaporating the water. The loss was mainly the portion stuck on the wall of flask. In a continuous operation, we believe that nearly 100% of NaCl can be regenerated and reused.

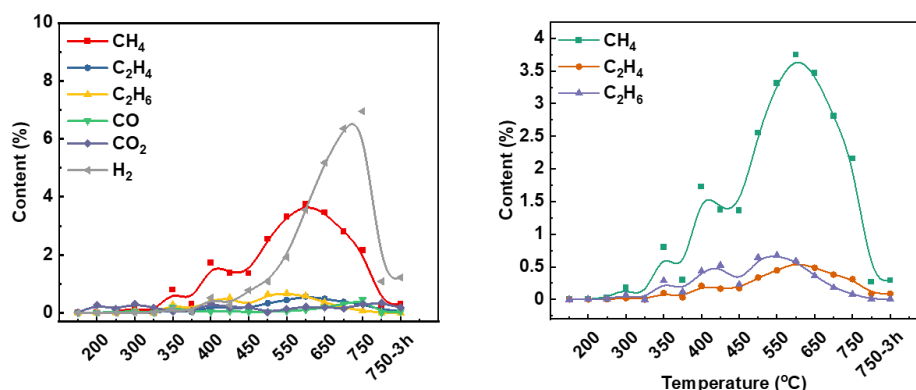


Figure 9. The emission during carbonization characterized using the GC.

To identify the main emissions in the carbonization process, the exhaust gas was collected at various stage of carbonization and analyzed with gas chromatography. As showed in **Figure 9**, the emissions are mainly CH₄ and H₂, with small amount of CO₂ and CO, occurring between 450-750°C. After carbonization at 750 °C for 3 hours, the exhaust becomes mainly small amount of H₂. According to the integration of gases, the amount of CH₄ is roughly equal to H₂ in the whole process. Based on the elemental composition in asphaltene feedstock and the resulting ANC, there must be H₂S and NH₃ emissions because of the loss of S and N in the carbonization. However, the GC used in this work can not identify these two gases.

Taking the yield and elemental composition change in consideration, we list the estimated emissions in the carbonization process in **Table 2**. For instance, to produce 1 kg of ANS-20-900, the emissions are mainly 0.74 kg CH₄, 0.09 kg H₂, 0.1 kg H₂S and 0.01 kg NH₃. The results indicate the importance of treating the reusing the exhausts. In a large-scale production, H₂S and NH₃ will be captured by basic and acidic solution, while the CH₄ and H₂ will be reused to generate the heat for carbonization.

Table 2. The estimated emission in the production of ANS.

	Composition ^a			Yield %	Emission per kg ANS ^b			
	C %	S %	N %		CH ₄	H ₂	H ₂ S	NH ₃
Asphaltene	79.0	8.3	1.3					
ANS-20-900	90.4	5.3	1.4	54	0.740 kg	0.093 kg	0.107 kg	0.012 kg
ANS-20-1050	93.6	4.3	1.2	53	0.738 kg	0.092 kg	0.121 kg	0.015 kg
ANS-20-1200	93.8	3.1	0.9	52	0.775 kg	0.097 kg	0.136 kg	0.019 kg

Note: ^a The weight percentage; ^b assuming the emission is in form of CH₄, CH₂, H₂S and NH₃.

The ANC products were fabricated via a two-step carbonization process. Asphaltene supported on NaCl was carbonized at 750°C in the first step and resulting carbon (after removing NaCl) was further annealed to desired temperature (e.g., 900 °C) in the second step. Given the relatively low heat capacity of carbon (0.71 J/g K), the energy consumption of carbonizing asphaltene itself will be only a very small portion of

the total cost. The estimated cost should be similar to the biochar that is priced at \$2-3 USD/kg. The extra energy cost comes from heating NaCl in the first carbonization step as the mass of NaCl is much higher than asphaltene. Considering the heat capacity of NaCl (0.86 J/gK) and the production yield of 55%, an extra energy of 22,672 kJ or 7.3 kWh is required to heat the NaCl in the production of 1kg ANC-20 sample. With the current electricity price of ~ \$ 0.1 CAD/kWh in Alberta, that will be an extra cost of \$ 0.73 CAD. To produce 1 kg thin ANC-500, the NaCl heating cost will be \$18.25 CAD. Clearly, the quality (performance) and cost of ANC need to be carefully balanced in the next phase development.

Another major production cost is related to the ball milling process that refines the NaCl, provide more adsorption surface and creates edges. A small high energy planetary ball mill was used in this project. It is difficult to estimate the real energy cost based on this small equipment. Instead, we did a set of experiments to evaluate the impact of milling time on the resulting performance ANC. In a typical experiment, the asphaltene/NaCl was ball milled for a total of 800 minutes (80 cycles, 10 minutes/cycle and 5 minutes resting between cycles). **Figure 10** shows the ANC-20 produced by ball milling 400 minutes (40 cycles), 120 minutes (12 cycles), 60 minutes (6 cycles) and 30 minutes (3 cycles).

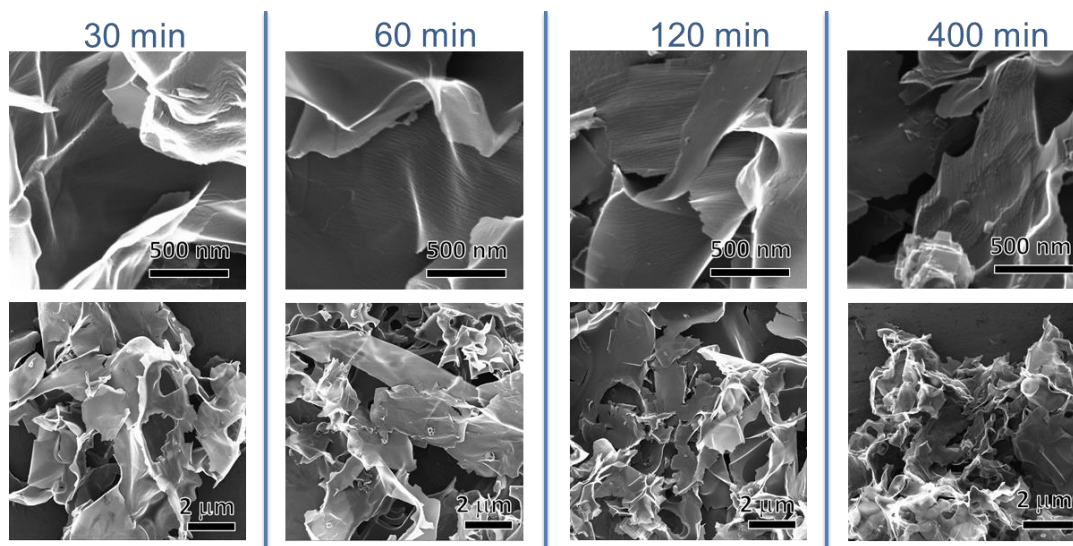


Figure 10. The ANC-20-750 processed various ball milling time.

Although carbon nanosheets was achieved in all the experiments (**Figure 10**), the milling time greatly impact the electrochemical performance as showed in **Figure 11**. ANC-20 prepared with short ball milling cycles performances similar to the directly carbonized sample without NaCl template (DCA-900). Clear advantage over DCA-900 was observed when the milling time reaches 400 minutes (40 cycles) As the SEM images demonstrated, longer ball milling time enhances fragmentation, leading to thinner carbon nanosheet structures and enlarged surface area, which boost the K-storage capacity.

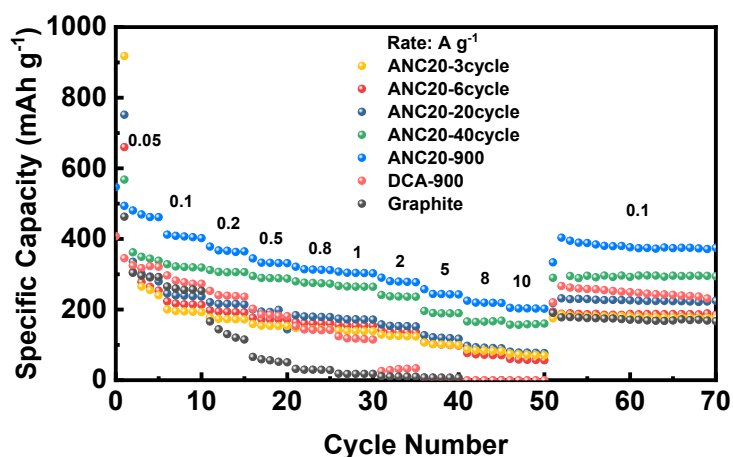


Figure 11. The K-storage performance of ANC-20 processed with different ball milling time.

To explore the possibility of deriving the ANC on large scale, a rolling mill (tumbling mill) is utilized instead of the planetary ball mill. In a typical experiment, 800 g NaCl, 40 g of asphaltene, and 80 mL toluene were placed in a 3-liter steel bowl together with 30 steel milling balls ($d=80$ mm) and processed at 75 RPM for 800 minutes continuously on a rolling mill (**Figure 12a,b**). No free running liquid was observed after milling. The as-prepared samples were dried in the fume hood after the ball milling finished (**Figure 12c**). Comparing with the high-energy planetary ball mill, the rolling mill inputs much lower energy to the milled materials, but the large-sized steel balls provide fraction impacts. The SEM images reveal the porous structure of ANCRM20 (**Figure 12d**). However, the zoomed-in images (**Figure 12e,f**) illustrate the macropores (~ 200 nm) as the result of the removal of the fractured NaCl templates. Compared to the morphology of the ANC20, there are rarely “stripe-like” nanostructures on the carbon sheets on ANCRM-20.

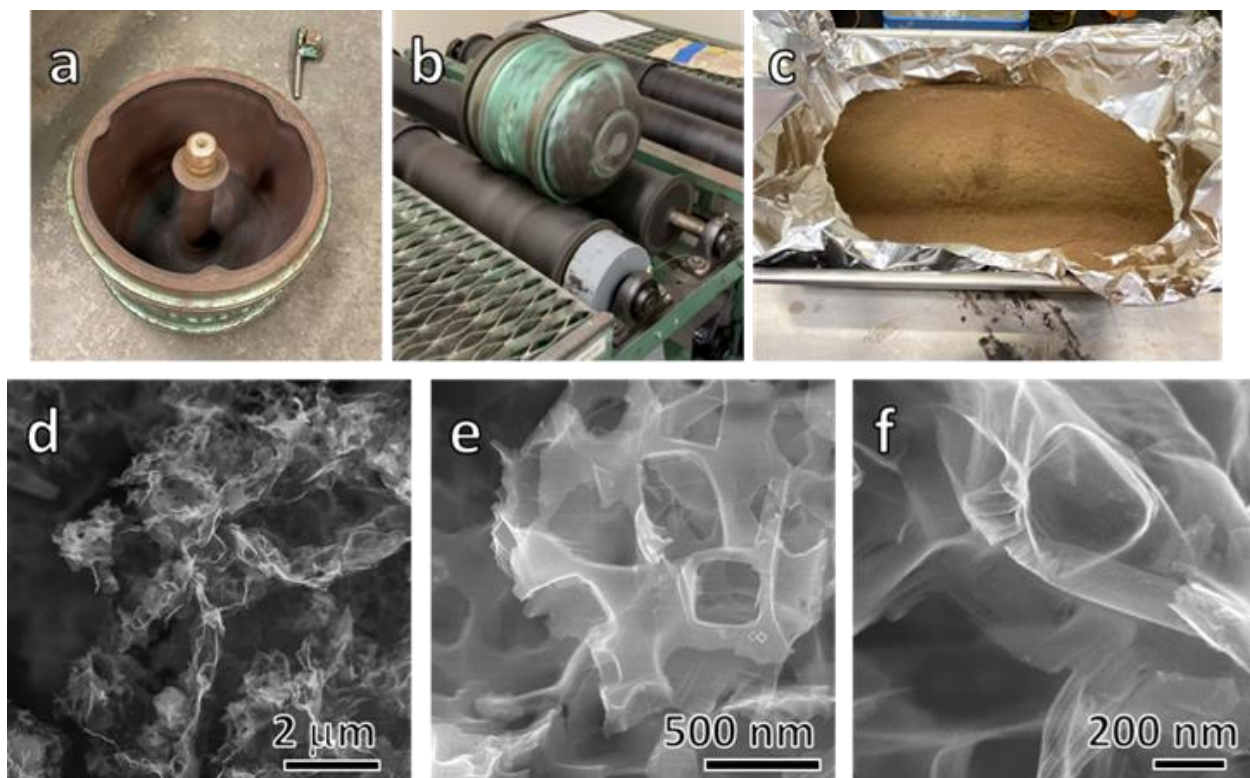


Figure 12. Images of a) rolling mill jar, b) rolling mill, and c) the as derived ANCRM; d) SEM image of ANCRM20; e) and f) zoomed-in SEM images of ANCRM20.

5. **Additional results:** the carbon nanosheets templated from Na_2CO_3 for Li-S batteries

Following the success of the edge-rich asphaltene-derived nanocarbon with NaCl templates, we further explored the effects of the templates. As we reported before, a group of thermal-stable, low-cost, and water-soluble chemicals had been employed as candidates to generate carbon nanostructure via the ball milling approach. Among them, sodium carbonate (soda, Na_2CO_3) as a monoclinic crystal with a melting point of 851°C and a solubility of 30g (in 100mL water at 20°C) is an outstanding template delivering graphene-like carbon with three dimensional (3D) nanoporous structures from the asphaltene precursor (denoted at ANCS20, with asphaltene/template ratio of 1/20). Differs from the NaCl template, Na_2CO_3 decomposes slowly at the temperature higher than 400°C during the carbonization process, releasing CO_2 gas. The CO_2 acts as a chemical activation agent reacting with the carbon nanosheets covered on the templates, which creates additional porous structures and expands the surface area, resulting in the 3D nanoporous carbon (**Figure 13a, b**). TEM and high-resolution TEM images illustrate the 3D porous structure consisted by the nano-thin carbon sheets (**Figure 13c, d**). The HR-TEM further reveals the short-range order of the ANCS20 nanosheets. Compared to that of AN20, the ANCS20 has a much-increased surface area and pore volume (**Table 3**). Besides, the ANCS20 demonstrates a wide range of pore sizes from 3 nm to 30 nm, indicating the multi-step mesopore formation mechanism including the template effect and the CO_2 activation.

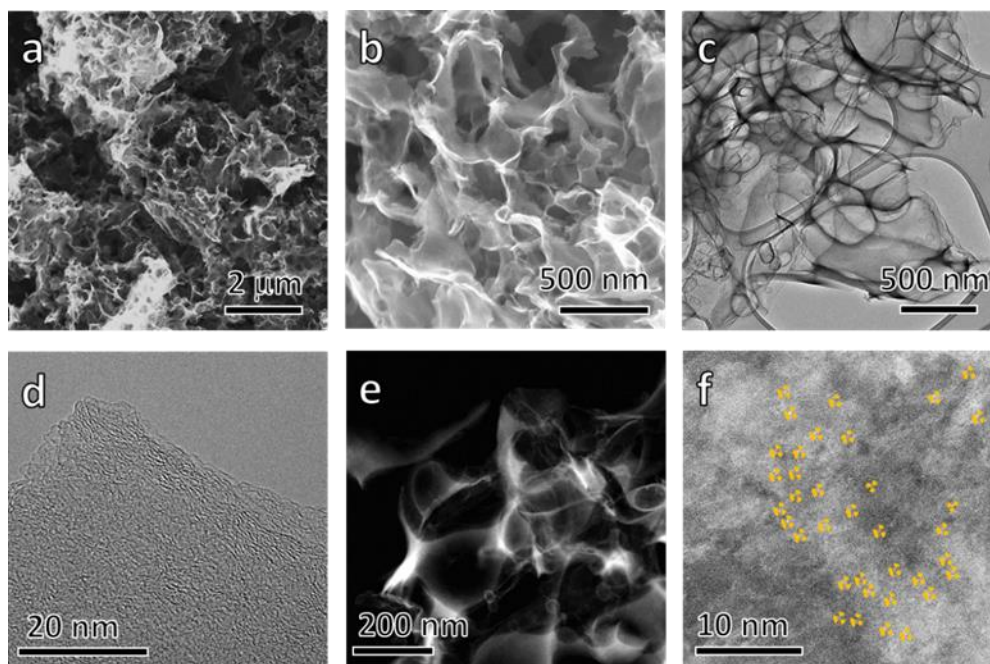


Figure 13. Electron microscopy images of ANCSD20: a) and b) scanning electron microscopy (SEM) images of ANCSD20; c) and d) transmission electron microscopy (TEM) and high-resolution TEM (HR-TEM) images of ANCSD20; e) and f) Aberration-corrected high-angle annular darkfield scanning transmission electron microscopy (AC-HAADF-STEM) images.

Aberration-corrected high-angle annular darkfield scanning transmission electron microscopy (AC-HAADF-STEM) further demonstrates the 3D porous nature of the ANCSD20, which consists of thin graphene-like carbon sheets (**Figure 13e**). The naturally existing single-atom catalytic (SAC) sites are also reserved on the ANCSD20 (**Figure 13f**), which is similar to the SACs on the previously reported ANC20. Yet, we hypothesises the porous structure and the enlarged surface area could further enhance the catalytic activity of ANCSD20. All these properties promote ANCSD20 as a catalyst for high-performance lithium-sulfur (Li-S) batteries.

Table 3. Surface area and pore volume of ANCSD20, ANC20, and DCA

Samples	Surface Area (m ² g ⁻¹) ^a	Total Pore Volume (cm ³ g ⁻¹) ^b
ANCSD20	511	1.16
ANC20	187	0.28
DCA	7.9	0.012

a. The specific surface area was calculated with Brunauer-Emmett-Teller (BET) methods; b. the total pore volume was determined at a relative pressure of 0.95.

Li-S batteries with high capacity (1650 mAh g^{-1}) and high energy density (2600 Wh kg^{-1}) are drawing increasing attention. However, the free-migration of the polysulfides (PSs) intermediates between the anode and cathode, known as the “shuttle effect”, leads to irreversible sulfur consumption and anode passivation, resulting in poor cycle life of the Li-S batteries. A suitable interlayer material that could reduce PSs permeation is expected to suppress the “shuttle effect” and stabilize the sulfur electrochemistry. In this work, ANCSD20 is employed as the interlayer in addition to the polypropylene separator (Celgard). The porous surface and the naturally existing SACs are capable of the synergic reservoir and stabilize the PSs. The ANCSD@Cel separator was prepared by simply casting the slurry containing the ANCSD20 and polyvinylidene fluoride (PVDF) in weight ratio of 9:1 in 1-methyl-2-pyrrolidinone (NMP) solvent onto the conventional Celgard membrane, and dried at 60°C overnight.

The ANCSD20 has a similar initial capacity at the 0.1C activation cycles compared to the Super P cell. However, at 1C rate, ANCSD20 demonstrates higher capacity, indicating the enhanced sulfur utilization (**Figure 14a**). The capacity decay of ANCSD20 cell is minimized compared to the Super P cell. After 200 cycles, the ANCSD20 retains 83% of its initial capacity and after 450 cycles the capacity of the ANCSD cell is still twice as high as that of the Super P cell (574 vs. 236 mAh g^{-1}). Comparing the galvanostatic charge-discharge (GCD) profile of the two cells (**Figure 14b, c**), the ANCSD20 has a much larger low plateau in the discharge curve, showing the ANCSD20 elevates the PSs conversion into the final product of $\text{Li}_2\text{S}_2/\text{Li}_2\text{S}$. Also, the low plateau of ANCSD20 turns into a slope, indicating the PSs conversion reaction kinetics affected by the ANCSD, which is possibly related to the SACs on the ANCSD20. The mesoporous ANCSD20 performed as a sulfur reservoir and the high surface area provides additional active catalytic sites for PSs conversions. Thus, the synergetic effect of the ANCSD20 enhanced the Li-S battery capacity and stability at higher rates (1C). However, to further understand the enhancement mechanism, additional electrochemical and characterization is in process.

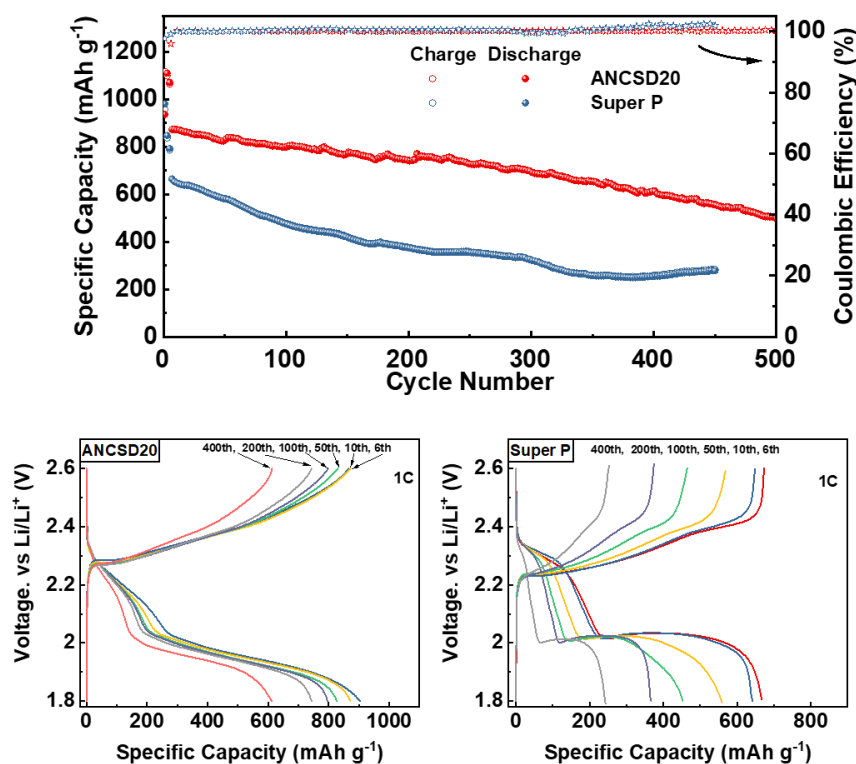


Figure 14. Electrochemical performance of ANCSD20 as S host for Li-S battery: a) the stability of ANCSD20-based Li-S cell in comparison with typical carbon black (Super P)-based Li-S cell; b) and c) the charge/discharge curves of Li-S cell based on ANCSD20 and Super P at various cycles.

F. KEY LEARNINGS

Please provide a narrative that discusses the key learnings from the project.

- Describe the project learnings and importance of those learnings within the project scope. Use milestones as headings, if appropriate.
- Discuss the broader impacts of the learnings to the industry and beyond; this may include changes to regulations, policies, and approval and permitting processes

RESPOND BELOW

• Adsorption limit/thickness limit

Our scientific goal is to achieve as thin as possible carbon nanosheets for the maximal value, ideally with thickness less than 2 nm, or even single-layer graphene. Due to the poor affinity between asphaltene and NaCl crystals, it will be very challenging to fabricate carbon nanosheets thinner than 2nm by just reducing asphaltene: NaCl ratio. **Figure 15** shows the morphology of ANC-1000-750, with asphaltene: NaCl ratio of 1: 1000. This is 5 times less asphaltene compared to the sample ANC-200-750 shown in **Figure 3**. At this

ratio, we start to see more incomplete carbon nanosheets with large holes (**Figure 15a**), indicating the partial coverage of asphaltene on the NaCl surface. Some of the striped features even become detached. **Figure 15b** shows a large striped carbon nanosheet with several carbon cages on top. **Figure 15c** shows the high-resolution TEM of the marked area with three carbon cages. In the background, the 4 stripes from the carbon nanosheets below can be observed. The middle cage notably tilts away from the beam direction, while the edges of the left and right cages are roughly in the beam direction with a thickness of 2.5 nm and 1.8 nm. The thickness of carbon nanosheets is estimated in a similar range.

Judged on the TEM and BET surface area results, we believe 1:1000 is already approaching or surpassing the lower limit of asphaltene: NaCl ratio to achieve a complete coating. The lower thickness limit of resulting carbon nanosheets is in the range of 1.5-3 nm. By further optimizing the processing conditions (e.g., the ball milling parameters), carbon nanosheets with thickness around 2nm might be achieved. However, the NaCl system may not be suitable for ultrathin carbon nanosheets less than 1 nm (1-3 layers), which requires a substrate with a stronger affinity with asphaltene.

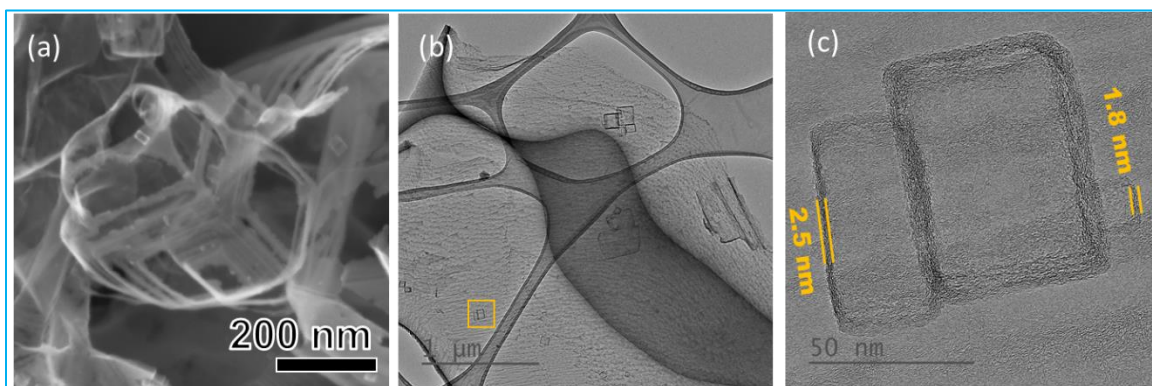


Figure 15. The morphology of ANC-1000-750 by templating NaCl (asphaltene: NaCl = 1: 1000 by weight). The SEM image shows the incomplete carbon nanosheets with holes (a); TEM images show a large striped nanosheet overlapped with several carbon cages (b) and 3 carbon cages in the marked area.

The electrochemical performance of carbon nanosheets with different thicknesses is shown in **Figure 16**. The ANC-1000-750 sample with the highest specific surface area exhibits the best performance for both Na-ion and K-ion batteries. Interestingly, the thickest ANC-20-750 sample delivers remarkably better performance than ANC-200-750. The ANC-200-stir-750 sample was prepared by adsorption and filtration without ball milling. It shows the lowest capacity among carbon nanosheets. The thickness has a significant impact on the electrochemical performance. For a fair comparison, all the carbon nanosheets are carbonized at 750°C without further annealing.

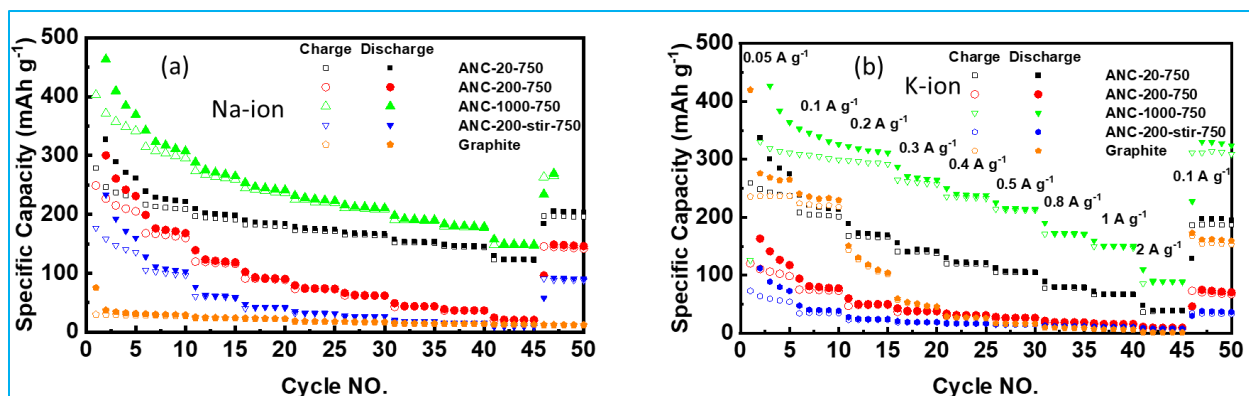


Figure 16. Electrochemical performance of carbon nanosheets prepared with different asphaltene: NaCl ratio for Na-ion battery (a) and K-ion battery, in comparison with commercial graphite. All the samples were carbonized at 750°C without further annealing.

- **Edge-rich features: strips and cages**

Graphite can be visualized as a stack of hexagonal nets of carbon atoms (graphite layer). The carbon atoms in the same layer are connected by strong σ -bonds (0.142 nm) in hexagonal, while the adjacent layers are connected by weak π -bonds (0.335 nm). The plane perpendicular to the graphitic layer is named as edge plane with characteristic large lattices distance of 0.335 nm. The edge plane sites have received great attention in electrochemical catalysts because the edges and defects are more active than the basal plane. The large lattice distance also facilitates the fast ion intercalation for battery application.

Regardless of asphaltene: NaCl ratio, all carbon nanosheets templated from NaCl show striped structures. **Figure 17a** highlights the uniform stripes on carbon nanosheets ANC-200-850. This sample is similar to the one shown in **Figure 3** but annealed at a higher temperature (850°C). From the HR-TEM analysis (**Figure 17b**), it can be concluded that the parallel stripes are ~ 3.5 nm wide and ~ 10 nm from each other. Most interestingly, all the stripes are edge plane sites, with lattices distance of ~ 0.34 nm. Compared to typical few-layer graphene, the carbon nanosheets possess much more edge plane sites. To the best of our knowledge, there are no carbon nanomaterials with a comparable amount of edge plane sites in the open literature. **Figure 17c** shows the typical carbon cubic nanocages templated from NaCl nanocrystal. Although there are no stripes on the nanocages, their small size also provides plenty of edges.

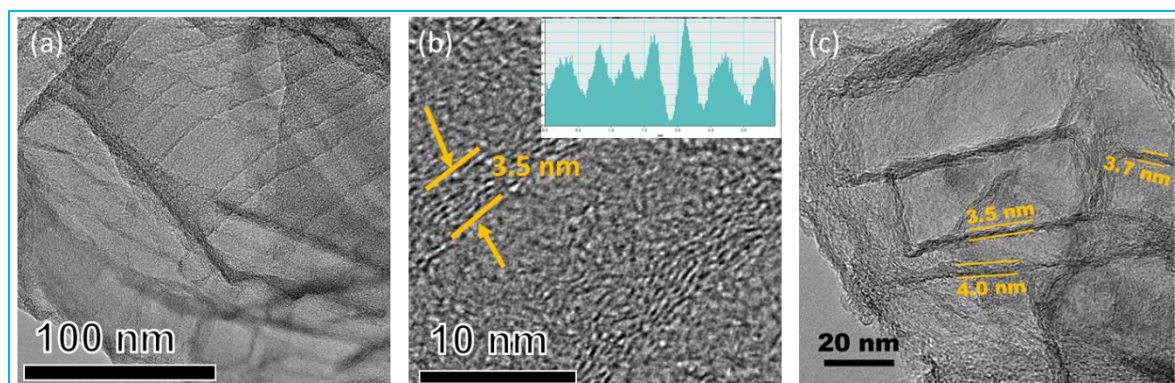


Figure 17. The edge-rich features in ANC-200-850 by templating NaCl (asphaltene: NaCl = 1: 200). The SEM image (a) and TEM image (b) of the striped structure on carbon nanosheets; The TEM image of small cages, templated from small NaCl crystal.

We employed the density function theory (DFT) to elucidate the role of edges and S in energy storage. We developed few-layer carbon models containing carbon edges, defects (carbon vacancies) and sulfur heteroatom to estimate the K-ion adsorption energy (E_{ads}) on the ANC on three sites as the edges, basal planes and intercalated in carbon layers. The K-ion adsorption and the corresponding adsorption energies are illustrated in **Figure 18a**. Comparing all the adsorption energies simulated, we can conclude that the edge plane is the most favorable adsorption site for K-ion with E_{ads} varies from -2.78 to -2.71 eV for all the calculated models, which are much lower than that of the K-ion intercalation. In both models with single vacancy and sulfur dopant, adsorption energy on basal planes (-2.43 and -1.68 eV, respectively) on carbon surface is lower than that of the non-defected carbon (-1.53 eV), indicating an elevated K-ion surface binding with carbon defects and hetero atoms. All the simulation results suggest that the edge planes and surfaces are dominant binding site for K storage, which indicates a high capacity in the high voltage region in the electrochemical K-storage process. Besides, the defects and sulfur hetero atom both promote the K-ion intercalation in carbon interlayers, which contributes to the total K-storage capacity.

We further estimated the K-ion diffusion pathways on ANC. The energy favorable edge site is selected as the K-ion starting point and the energy barriers on three possible migration pathways are simulated using the climbing image-nudged elastic band (CI-NEB) method (**Figure 18b**). As illustrated in **Figure 18c**, the K-ion migrates along the carbon edges with the lowest resistance, while the intercalation ought to overcome the highest energy barrier. Similar with the adsorption energy results, the sulfur hetero atom and carbon vacancy decrease the K-ion migration energy barrier compared to the non-defected carbon, promoting the K-storage kinetics. Comparing with previous carbon anodes, the edge-rich and defected ANC is more preferable for K-storage.

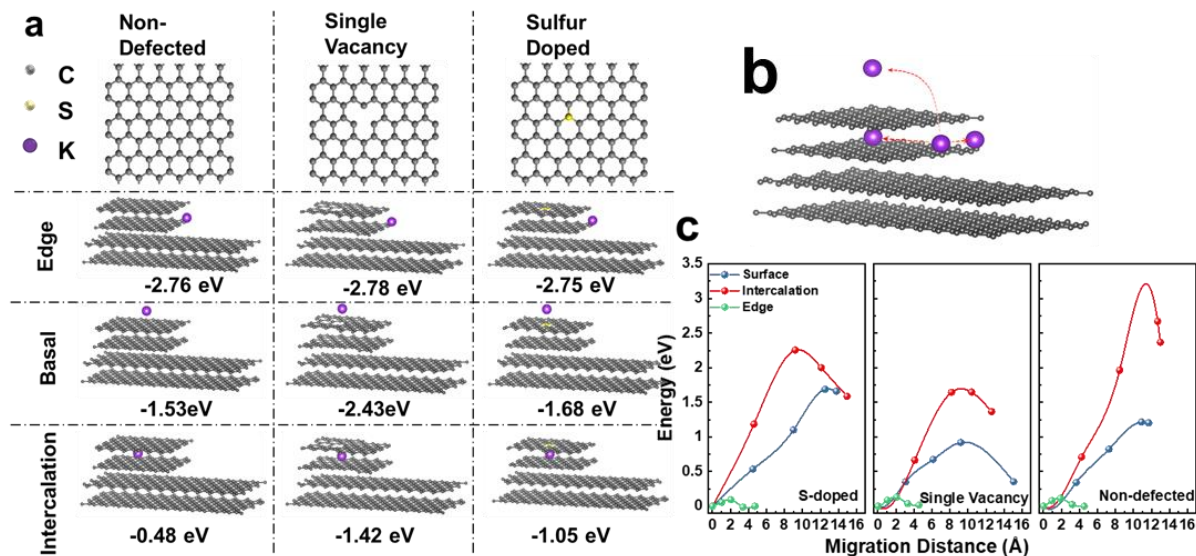


Figure 18. DFT simulated ANC structures, K-ion binding energy and migration pathways. a) optimized K-ion adsorption on different sites of the edge-rich carbon structure with possible carbon vacancies and sulfur heteroatom: on the edge; on the basal plane and intercalated into carbon layers; b) a schematic illustrating the K-ion migration pathways: along the edge; onto surface plane and intercalation into carbon layer; c) energy barrier of the K-ion migration estimated by CI-NEB method on the sulfur doped, single vacancy and non-defected edge-rich carbons.

• Ball milling conditions

Ball milling is an environmentally friendly and cost-effective technique widely used in industry to grind powders into fine particles and blend materials. The Fritsch Pulverisette 6 planetary ball mill used in this project and the working mechanism are shown in **Figure 19a, b**. During the ball milling process, the collision between the grinding balls generates localized high shear or compressive forces to the materials on the surface of balls. The NaCl is refined into small crystals with more surface area to adsorb asphaltene. The compressive force provides a cold-welding effect, which can enhance the bonding between asphaltene and NaCl. Meanwhile, the shear force removes the excess asphaltene and reduces the thickness of the asphaltene layer.

The ball milling conditions are essential to the quality of final products. For instance, heavy grinding balls will provide larger forces that may help to further reduce the thickness of resulting carbon nanosheets. **Figure 19c-d** and **Figure 19e** shows the morphology of carbon processed with tungsten carbide and stainless-steel balls. The tungsten carbide balls lead to carbon nanoplatelets and the stainless-steel balls result in nanoporous carbon, indicating the NaCl crystals were broken into particles by the heavy balls that are too small to be used as templates to make carbon nanosheets.

To elucidate the role of ball milling, we designed a control experiment, where NaCl is ball milled first at the condition but without asphaltene to achieve refined NaCl. Then the refined NaCl was mixed with

asphaltene solution (1g asphaltene in 100 mL toluene). The mixture was refluxed at the boiling point of toluene for 4 hours under vigorous stirring before the toluene was completely removed by distillation. In that case, the ball milling plays only one role: refining the NaCl particle size, and the asphaltene was adsorbed on the NaCl surface without the help of ball milling. **Figure 19f** shows the SEM image of ANC obtained via the reflux-adsorption process. The resulting ANC is much thicker than the ANC prepared by ball milling NaCl and asphaltene together (ANCAD-20), indicating the aggregation of asphaltene on the NaCl surface. Interestingly, no stripes were observed in the ANC. **Figure 20** shows that the thick ANC prepared by the reflux-adsorption possesses significantly lower electrochemical performance in K-storage than the ANC prepared by ball milling NaCl and asphaltene together. At a low current density of 0.1 A g⁻¹, the different is about 30% and at a high current of 10 A g⁻¹, the different increases to around 200%.

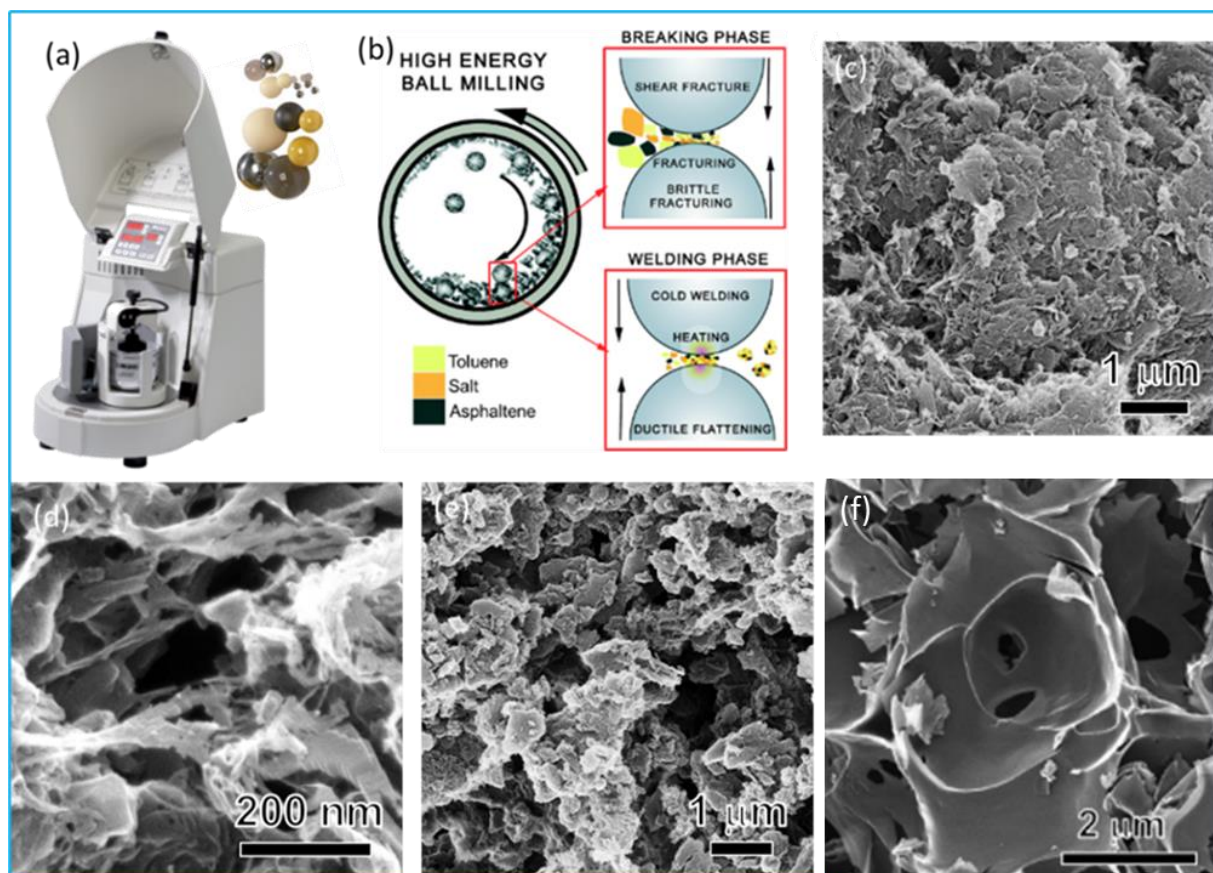


Figure 19. The role of ball milling. (a) The Fritsch Pulverisette 6 ball mill used in this project; (b) The interaction of asphaltene and salts in ball milling; The SEM images of NaCl templated carbon processed using tungsten carbide (c, d) and stainless-steel (e) grinding balls. (f) ANC-20 samples prepared by ball milling NaCl and reflux-adsorption (ANCAD-20). All the samples are prepared with asphaltene: NaCl of 1:200 and carbonized at 750°C.

As discussed in previous section, it is possible to fabricate ANC using rolling ball mill, which has much less energy input compared to planetary ball mill. However, the sample prepared by rolling mill (ANCRM20)

demonstrates a similar K-storage capacity as the ANCAD-20 until the rate is higher than 5 A g^{-1} (Figure 20a). The reduced rate performance of ANCRM20-900 can be attributed to the reduced surface area and edge-plane density, which barriers the K-ion diffusion and reduces the K-ion binding sites. Compared to that of ANC20, the GCD profiles of ANCRM20 at various rates (Figures 20 b, c) further reveal the capacity reduction in the 1.1 to 0.4V region, which corresponds to demoted K-ion surface binding, resulting from the low surface area and binding sites. However, the ANCRM20 demonstrates much improved K-storage capacity than the direct carbonized asphaltene (DCA-900) and commercial graphite, especially at a high rate. As such, the ANCRM derived via rolling mill is a potential candidate for scaling-up production.

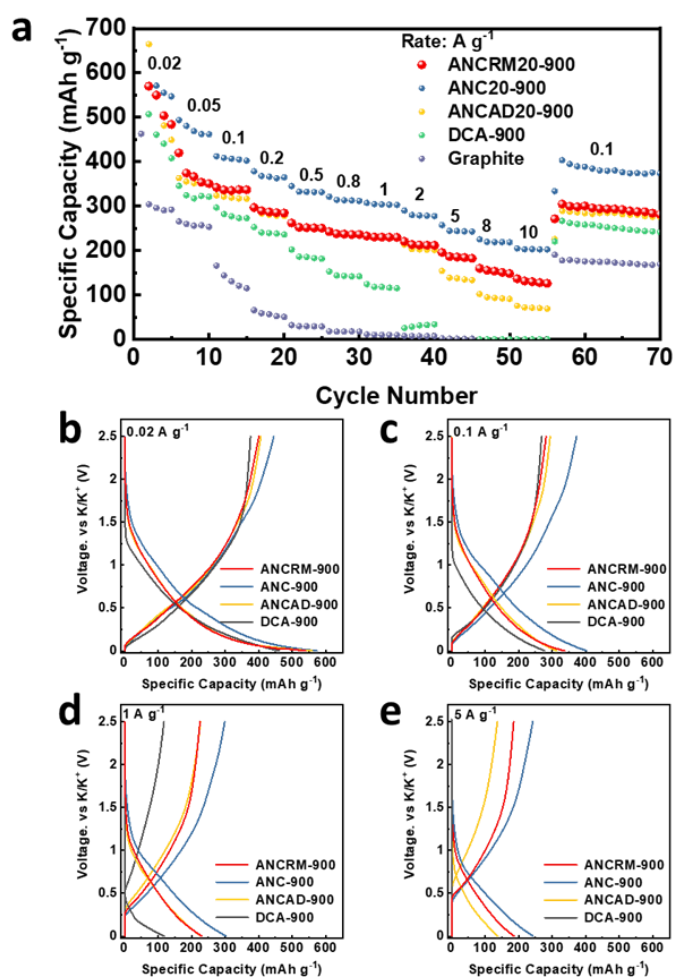


Figure 20. Electrochemical K-storage performance of ANC anodes: a) rate performance of ANCRM20-900, ANC20-900, ANCAD20-900 and DCA-900 anode materials; galvanostatic charge/discharge profiles at various rates: b) 0.02 A g^{-1} , c) 0.1 A g^{-1} , d) 1 A g^{-1} and e) 5 A g^{-1} .

- The role of toluene in ball milling

The role of toluene in the ball milling process could be two-folded: solvent for asphaltene and lubricant in milling. We found the amount of toluene is critical to the quality of the resulting carbon nanosheets. Initially, we use 10ml toluene to process 1g asphaltene. We systematically studied the role of toluene by adding 10, 4, 2, 1, and 0 (dry milling) mL toluene in ball milling 1g asphaltene and 20g NaCl. In a control experiment, 10 mL pentane was used as milling lubricant since asphaltene is insoluble in pentane. As shown in **Figure 21**, even without toluene or with pentane, carbon nanosheets can still be prepared. But the resulting carbon sheets are significantly thicker than the ones processed with toluene.

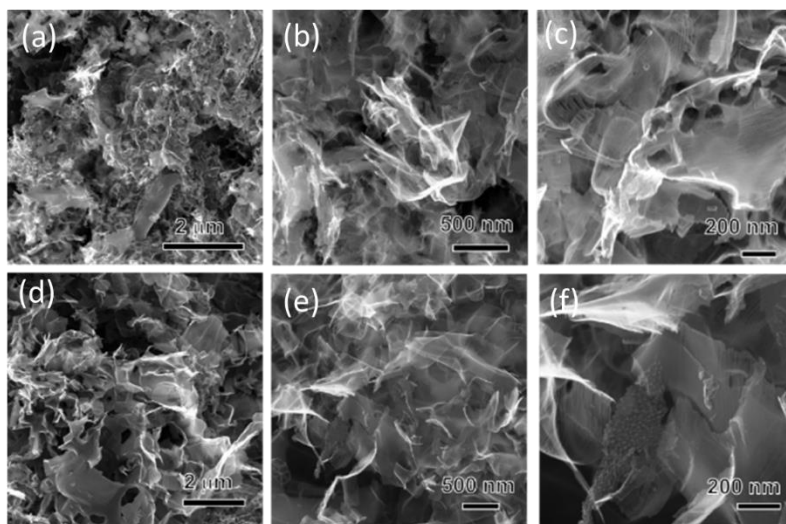


Figure 21. The ANC processed without any solvent (a-c) and with pentane (lubricant) in ball milling (d-f).

Figure 22 shows the K-storage performance of ANC prepared using different amounts of toluene. Overall, all the samples processed with toluene have better performance than the ones without toluene or with pentane, suggesting the toluene promotes the formation of high-quality carbon nanosheets mainly by dissolving asphaltene, rather than lubricating the milling process. To process 1g asphaltene, the optimal toluene amount is identified to be 4mL. We believe the optimal amount of toluene is likely related to the viscosity of the asphaltene/toluene solution. Asphaltene solution of 0.25g asphaltene in 1 mL toluene possesses the suitable viscosity to form a uniform coating on the NaCl surface in the ball milling process.

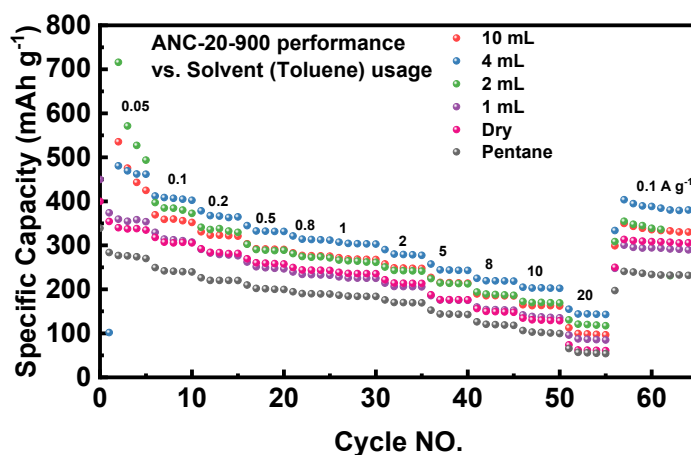


Figure 22. The K-storage performance of ANC processed with different lubricants in ball milling.

- **The edge-rich ANC as substrate for Pt catalysts**

Besides the application in batteries, ANC can also serve as a substrate for electrocatalysts. Two Pt catalysts were prepared using ANC-200-750 as substrate. Pt NP@ANC750 stands for Pt nanoparticles (20% Pt) supported on carbon nanosheets, and Pt-SA@ANC750 represents Pt single atoms (1% Pt) dispersed on carbon nanosheets. As shown in **Figure 23a-c**, the Pt single atoms are only observable at high-resolution TEM. A high concentration of Pt atoms can be found on the edge-rich defects.

Figures 23d-f display the electrochemical oxygen reduction activity of ANC-supported Pt catalysts compared with a Pt/carbon commercial catalyst with 20% Pt (Sigma). The Pt nanoparticles supported on ANC shows similar performance to commercial Pt/carbon catalyst, promoting a 4-electron transfer reaction ($\text{O}_2 + 2\text{H}_2\text{O} + 4\text{e}^- \rightarrow 4\text{OH}^-$). In contrast, the Pt single atoms catalyst boosts the 2-electron transfer process forming hydroxide ($\text{O}_2 + \text{H}_2\text{O} + 2\text{e}^- \rightarrow \text{HO}_2^- + \text{OH}^-$). More experiments are in process to evaluate the potential of Pt-SA@ANC750 catalyst in sustainable hydrogen peroxide production, especially the role of edge-rich defects. Nevertheless, it can be concluded from the existing results that the ANC can serve as conductive substrate for electrocatalysts.

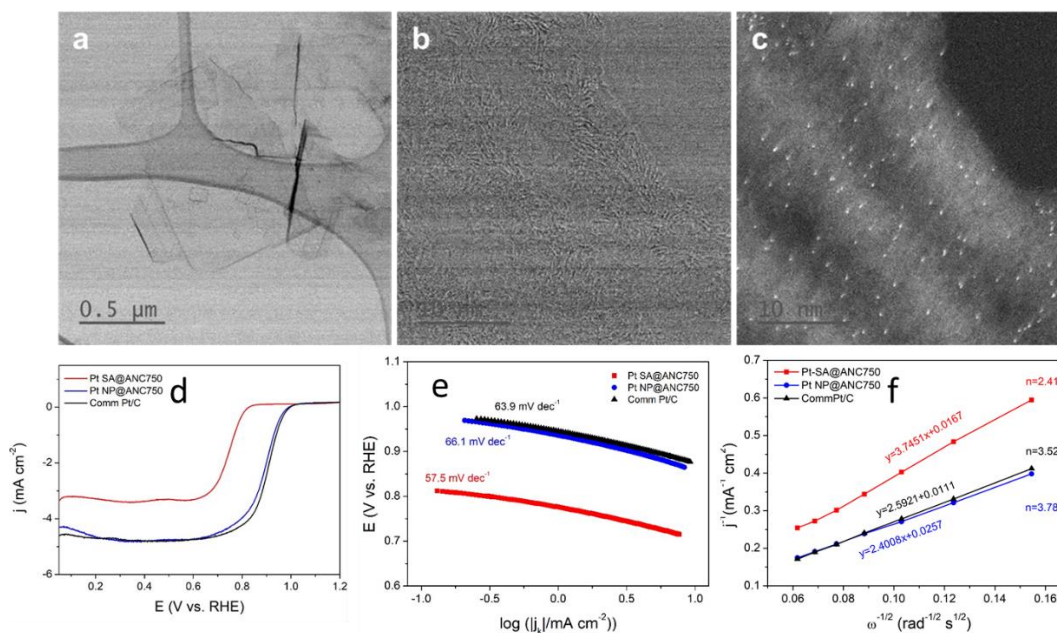


Figure 23. (a) TEM images of Pt SA@ANC750; (b,c) high-resolution BF-TEM and AC HAADF-STEM images of Pt SA@ANC750; (d) ORR polarization curves with a scanning rate of 5 mV s^{-1} for the synthesized catalysts in 0.1 M KOH solution at 1600 rpm . (e) Tafel slopes for these catalysts. (f) Koutecky-Levich plots of the synthesized catalysts at 0.6 V vs. RHE.

G. OUTCOMES AND IMPACTS

Please provide a narrative outlining the project's outcomes. Please use sub-headings as appropriate.

- **Project Outcomes and Impacts:** Describe how the outcomes of the project have impacted the technology or knowledge gap identified.
- **Clean Energy Metrics:** Describe how the project outcomes impact the Clean Energy Metrics as described in the *Work Plan, Budget and Metrics* workbook. Discuss any changes or updates to these metrics and the driving forces behind the change. Include any mitigation strategies that might be needed if the changes result in negative impacts.
- **Program Specific Metrics:** Describe how the project outcomes impact the Program Metrics as described in the *Work Plan, Budget and Metrics* workbook. Discuss any changes or updates to these metrics and the driving forces behind the change. Include any mitigation strategies that might be needed if the changes result in negative impacts.
- **Project Outputs:** List of all obtained patents, published books, journal articles, conference presentations, student theses, etc., based on work conducted during the project. As appropriate, include attachments.

RESPOND BELOW

1. Project Outcomes and Impacts:

In this project, we developed a low-cost procedure to convert asphaltene into graphene-like materials. Two types of graphene-like carbon nanosheets were derived from asphaltene by employing NaCl and Na₂CO₃ as templates. The resulting materials show excellent performance in various energy storage applications. The asphaltene-derived carbon nanosheet sheds light on the bitumen beyond-combustion applications with a cost-effective and sustainable derivation approach, leading to the conversion of petroleum industry products to sustainable energy storage materials.

2. Clean Resources Metrics:

- \$ in Innovative Production and Distribution: 345,000

As planned, a total of \$345,000 was utilized to develop the innovation, including the contribution from Alberta Innovates, NSERC, and IOSI.

- TRL advancement: 2

At the beginning of the project, the TRL of the technology is 2. We formulated the concept of fabricating carbon nanosheets by carbonizing the asphaltene adsorbed on salts based on findings in preliminary experiments. In the project, we have developed a procedure to make defects-rich carbon nanosheets based on two scalable processes: ball milling and carbonization. We have systematically studied the impact of salts, milling conditions, the asphaltene/salt ratio, and carbonization temperature on the morphology of carbon nanosheets and their electrochemical performance. Till now, we have achieved a TRL of 4, with the demonstrated proof of concept and validated application of ANC in a laboratory environment.

- # Students (Msc., PhD, Postdoc): 2

Two postdocs have been employed and trained in the project.

- # of Publications 3

To improve the quality of the research paper, we used the synchrotron facility at Canada Light Source and also DFT modeling to understand the mechanism. So, there is a delay in publication. We have one manuscript ready to submit, based on the NaCl templated ANC. There are two manuscripts under preparation regarding ANC as a conductive substrate for Pt single atom catalysts and the partially activated carbon nanosheets based on Na₂CO₃ templates for Li-S battery application.

Patents filed

We are planning to submit a patent application for the defect-rich ANC at the end of the project. We are working on carbon nanosheets processed with a similar procedure but with different salts (e.g., NaCl, Na₂CO₃, NaHCO₃, KCl, K₂CO₃ and KHCO₃) and the different applications of the resulting carbon nanosheets so that the protection can be maximized in one patent application.

3. Program Specific Metrics:

- Unique product/process: demonstrate the production of graphene-like nanoplatelets from asphaltenes

In the project, we have developed a procedure to make defects-rich carbon nanosheets based on two scalable processes: ball milling and carbonization. The process can be scaled up to make ~6 g carbon nanosheets in one batch using lab equipment.

4. Project Success Metrics:

- Adsorption of asphaltene, layers/thickness: Few layers
Achieved.

- Quality of carbon nanosheets, thickness: 2-5 nm
Achieved.

- Productivity, production per batch: 10g

Limited by the size of the planetary ball mill, we can process 6 g ANC-20 carbon nanosheets per batch. By upgrading to a high-capacity mill, (e.g., Fritsch Pulverisette 5/4), the production per batch can be improved to 24g. In the experiments using tumbling ball mill, the productivity was improved to 20g/batch by processing 800g NaCl and 40 g asphaltene in one milling jar.

H. BENEFITS

Please provide a narrative outline the project's benefits. Please use the subheadings of Economic, Environmental, Social and Building Innovation Capacity.

- **Economic:** Describe the project's economic benefits such as job creation, sales, improved efficiencies, development of new commercial opportunities or economic sectors, attraction of new investment, and increased exports.
- **Environmental:** Describe the project's contribution to reducing GHG emissions (direct or indirect) and improving environmental systems (atmospheric, terrestrial, aquatic, biotic, etc.) compared to the industry benchmark. Discuss benefits, impacts and/or trade-offs.
- **Social:** Describe the project's social benefits such as augmentation of recreational value, safeguarded investments, strengthened stakeholder involvement, and entrepreneurship opportunities of value for the province.
- **Building Innovation Capacity:** Describe the project's contribution to the training of highly qualified and skilled personnel (HQSP) in Alberta, their retention, and the attraction of HQSP from outside the province. Discuss the research infrastructure used or developed to complete the project.

RESPOND BELOW

- **Economic:**

The project provides our industry partner with access to a new market: the ever-growing carbon nanomaterials market. This value-added usage of asphaltene also give our industry partner a significant edge in the competition on the global market. In the full commercialization stage, 50 new jobs will be created and a sale of \$30,000,000 is expected in 2030. Given the massive demand for high-quality carbon nanomaterials in USA and China markets, the advances achieved in the project will remarkably promote the export. In established full commercialization stage, we expect 80% of the total sales from international customers.

The resulting graphene-like carbon nanosheets can serve as a low-cost alternative of graphene and improve the energy storage efficiency, which in turn promotes the deployment of renewable electricity harvested from wind and solar. Since the proposed carbon nanosheets are a key component in energy storage devices, the project will likely stimulate the energy storage industry in Alberta and therefore further diversify the economy.

- **Environmental:**

Asphaltene contain significant amount of N and S heteroatoms. When burned, these heteroatoms are converted into harmful SO₂ and NO_x gases which cause acid rains and damage the ozone shield in atmosphere. In the proposed solution, we intend to preserve as much as possible N and S heteroatoms in the carbon because these heteroatoms can enhance the performance of carbon materials in supercapacitors and electrocatalysis. In short, the heteroatoms are employed to store more charges in the proposed carbon nanosheets rather than pollute our air.

- **Social:**

Canada is one of the leading nations in the research of renewable energy and energy storage. In Canada, over 50 megawatts (MW) of battery capacity is expected to be operational by 2018, dominating the total electricity storage market (81 %). The asphaltene-derived carbon nanosheets possess a unique positioning in this market sector. Petroleum byproducts is used in our proposed research as precursor for the electrode materials. This allows us to meet the energy storage challenges with minimal ecological footprint. The resulting carbon nanosheets are not only sustainable, but also cost-competitive compared to traditional carbon nanomaterials. The successful deployment of the proposed research will secure Canada's leading position in renewable electricity usage and create potential employment opportunities. In this proposed work, two HQPs will be trained as interdisciplinary researchers and future leaders for Canada's renewable energy and energy storage industry.

- **Building Innovation Capacity**

Training HQP is an integral part of our research philosophy. Attracting and training future science leaders is critical in translating science into economic prosperity. Several aspects of this research project ensured an extremely active intellectual environment conducive for fostering creativity. This program covers basic science to applied research to design and development of integrated systems. As part of the project, we trained two postdocs in the new area across petroleum science, nanomaterials and energy storage.

The two HQPs were trained as interdisciplinary researchers with expertise in material science, surface science, physics, chemistry and engineering, to think critically and offer creative solutions for real world applications. Under the supervision of PIs, the HQPs were responsible for executing research plan, collecting and interpreting data, preparing reports, and presenting the results to Imperial Oil. HQPs will also present the findings on international conferences and build up their own academic and industrial connections. Through this commercialization-oriented project involves both academia and industry, the HQPs built up valuable soft-skills in teamwork, communication, problem solving, leadership and interpersonal skills. In the Pilot plant stage, 5-10 HQPs will receive training thought the project. More HQPs (20-30) will be employed and trained at full commercialization stage.

I. RECOMMENDATIONS AND NEXT STEPS

Please provide a narrative outlining the next steps and recommendations for further development of the technology developed or knowledge generated from this project. If appropriate, include a description of potential follow-up projects. Please consider the following in the narrative:

- Describe the long-term plan for commercialization of the technology developed or implementation of the knowledge generated.
- Based on the project learnings, describe the related actions to be undertaken over the next two years to continue advancing the innovation.
- Describe the potential partnerships being developed to advance the development and learnings from this project.

RESPOND BELOW

In this project, the feasibility and scalability of converting asphaltene into graphene-like carbon nanosheets have been demonstrated at a lab scale. Given the unique structure (edge-rich, S doping and metal heteroatoms), excellent electrochemical properties and low processing cost compared to traditional graphene materials, we believe the developed carbon nanosheets possess high commercialization value. As a long-term goal, we are planning to commercialize the technology in Alberta in collaboration with industrial partners, providing the abundance of asphaltene and low energy cost in Alberta.

In the next two years, we are planning to build the pilot plant and scale up the production of carbon nanosheets to kilogram level per batch. After submitting the final report to IOSI, we will discuss with Imperial Oil about the plan for the next phase. Depending on the preference of Imperial Oil, we may include more industrial partners for the next phase.

J. KNOWLEDGE DISSEMINATION

Please provide a narrative outlining how the knowledge gained from the project was or will be disseminated and the impact it may have on the industry.

RESPOND BELOW

Due the restriction of pandemic, we don't have other communications, announcements, or media. besides the communication with the project advisor from Alberta Innovates and Imperial Oil. After submitting the final reports to AI and IOSI, we will present the results in domestic and international conferences.

K. CONCLUSIONS

Please provide a narrative outlining the project conclusions.

- Ensure this summarizes the project objective, key components, results, learnings, outcomes, benefits and next steps.

RESPOND BELOW

We have successfully developed a low-cost and scalable procedure to convert asphaltene into high-value graphene-like carbon nanosheets. The procedure involves 4 simple steps: i) coating asphaltene thin layer on the surface of water-soluble salts (NaCl or Na₂CO₃) via ball milling; ii) carbonizing asphaltene in a surface-confined mode at a temperature near to the melting point of salts; iii) dissolving the salts in water; iv) annealing the carbon at high temperature to achieve the desired graphitization degree. Compared to conventional graphene, these carbon nanosheets carry 3 unique advantages, which make the nanosheets very promising for energy storage applications. Firstly, the carbon nanosheets contains about 5% S, which alters the electron contribution and makes the carbon nanosheet electrochemically more active. Secondly, there are natural metal single atoms in the nanosheets, which provides additional catalytic activity. Thirdly, the structures of template salts provide the carbon nanosheets some unique features. When using NaCl as template, the resulting nanosheets process large amount of edge sites, which facilitate the ion intercalation and transportation. If the Na₂CO₃ was used as template, the resulting carbon nanosheets will possess a partially activated nanoporous structure, ideal for Li-S battery application. Considering the low-cost of asphaltene, the scalable, efficient and environmental-friendly ball-milling approach, the ANC nanosheets shed light on the sustainable way of converting the petroleum industry byproduct into energy storage materials and upgrading the petroleum industry into beyond-combustion era. Upon the completion of this project, we will discuss with our industry partner for a commercialization plan. In the next step, we are planning to scale up the process to a level of several kilograms per batch.